



OPEN ACCESS

EDITED BY

Maurizio Giustetto,
University of Turin, Italy

REVIEWED BY

Maria Amalia Di Castro,
Sapienza University of Rome, Italy
Andrea Marcantoni,
University of Turin, Italy

*CORRESPONDENCE

Ulf Strauss
ulf.strauss@charite.de

SPECIALTY SECTION

This article was submitted to
Cellular Neurophysiology,
a section of the journal
Frontiers in Cellular Neuroscience

RECEIVED 05 April 2022

ACCEPTED 13 July 2022

PUBLISHED 10 August 2022

CITATION

Döhne N, Falck A, Janach GMS,
Byvaltcev E and Strauss U (2022)
Interferon- γ augments GABA release
in the developing neocortex *via* nitric oxide
synthase/soluble guanylate
cyclase and constrains network
activity.
Front. Cell. Neurosci. 16:913299.
doi: 10.3389/fncel.2022.913299

COPYRIGHT

© 2022 Döhne, Falck, Janach,
Byvaltcev and Strauss. This is an
open-access article distributed under
the terms of the [Creative Commons
Attribution License \(CC BY\)](https://creativecommons.org/licenses/by/4.0/). The use,
distribution or reproduction in other
forums is permitted, provided the
original author(s) and the copyright
owner(s) are credited and that the
original publication in this journal is
cited, in accordance with accepted
academic practice. No use, distribution
or reproduction is permitted which
does not comply with these terms.

Interferon- γ augments GABA release in the developing neocortex *via* nitric oxide synthase/soluble guanylate cyclase and constrains network activity

Noah Döhne¹, Alice Falck¹, Gabriel M. S. Janach¹,
Egor Byvaltcev^{1,2} and Ulf Strauss^{1*}

¹Institute of Cell Biology and Neurobiology, Charité—Universitätsmedizin Berlin, Corporate Member of Freie Universität Berlin, Humboldt-Universität zu Berlin, Berlin, Germany, ²Institute of Neuroscience, Lobachevsky State, University of Nizhny Novgorod, Nizhny Novgorod, Russia

Interferon- γ (IFN- γ), a cytokine with neuromodulatory properties, has been shown to enhance inhibitory transmission. Because early inhibitory neurotransmission sculpts functional neuronal circuits, its developmental alteration may have grave consequences. Here, we investigated the acute effects of IFN- γ on γ -amino-butyric acid (GABA)ergic currents in layer 5 pyramidal neurons of the somatosensory cortex of rats at the end of the first postnatal week, a period of GABA-dependent cortical maturation. IFN- γ acutely increased the frequency and amplitude of spontaneous/miniature inhibitory postsynaptic currents (s/mIPSC), and this could not be reversed within 30 min. Neither the increase in amplitude nor frequency of IPSCs was due to upregulated interneuron excitability as revealed by current clamp recordings of layer 5 interneurons labeled with VGAT-Venus in transgenic rats. As we previously reported in more mature animals, IPSC amplitude increase upon IFN- γ activity was dependent on postsynaptic protein kinase C (PKC), indicating a similar activating mechanism. Unlike augmented IPSC amplitude, however, we did not consistently observe an increased IPSC frequency in our previous studies on more mature animals. Focusing on increased IPSC frequency, we have now identified a different activating mechanism—one that is independent of postsynaptic PKC but is dependent on inducible nitric oxide synthase (iNOS) and soluble guanylate cyclase (sGC). In addition, IFN- γ shifted short-term synaptic plasticity toward facilitation as revealed by a paired-pulse paradigm. The latter change in presynaptic function was not reproduced by the application of a nitric oxide donor. Functionally, IFN- γ -mediated alterations in GABAergic transmission overall constrained early neocortical activity in a partly nitric oxide-dependent manner as revealed by microelectrode array field recordings in brain slices analyzed with a spike-sorting algorithm. In summary, with IFN- γ -induced,

NO-dependent augmentation of spontaneous GABA release, we have here identified a mechanism by which inflammation in the central nervous system (CNS) plausibly modulates neuronal development.

KEYWORDS

IFN- γ , type-II interferon, cerebral cortex, neuroimmunology, phasic inhibition, MEA, NO

Introduction

IFN- γ , the only type-II IFN, is a pleiotropic inflammatory cytokine and contributes to immune defense against viruses, bacteria, and tumors (Kak et al., 2018). As a part of the adaptive and innate immune response, IFN- γ is mainly secreted by lymphocytes and functionally acts by influencing gene expression, protein synthesis, and induction of an antiproliferative state on most cell types by activating IFN- γ receptor and subsequently the JAK-STAT1 (Janus kinase–signal transducer and activator of transcription 1) pathway (Ivashkiv, 2018). IFN- γ is present in central nervous system (CNS) at baseline levels and is elevated in conditions, such as viral infections, CNS trauma, and cerebral ischemia (Monteiro et al., 2017). In the CNS, IFN- γ serves an important neuron-specific function (Clark et al., 2022), notably by enabling non-cytolytic viral clearance (Patterson et al., 2002).

Beyond its canonical role in controlling intracellular pathogens, a growing body of evidence suggests a direct impact of IFN- γ on the CNS. The absence of IFN- γ leads to neurodevelopmental abnormalities (Monteiro et al., 2015) that differ in healthy vs. inflammatory conditions (Litteljohn et al., 2014). Notably, some neuropsychiatric diseases, such as autism spectrum disorder (ASD; Saghazadeh et al., 2019) and depression (Schmidt et al., 2014), are associated with increased IFN- γ levels. Developmental disturbances due to withdrawal of care (i.e., maternal deprivation) also cause elevated IFN- γ levels as shown in hippocampus and prefrontal cortex of newborn rats (Giridharan et al., 2019) and intrauterine inflammation leads to the accumulation of IFN- γ -producing γ/δ T cells in the brain of fetal mice (Lewis et al., 2021). However, T cells of patients with schizophrenia exhibit decreased production of IFN- γ (Arolt et al., 2000), and the IFN- γ inducer Anaferon improved outcomes in schizophrenia therapy (Vetlugina et al., 2016). As many neuropsychiatric conditions display altered IFN- γ levels, and IFN- γ knockout produces changes in behavior and cognitive performance (for review Monteiro et al., 2017), taken together extant evidence indicates a possible role for IFN- γ in maintaining healthy brain function.

Moreover, IFN- γ has been reported to have fast-acting neuromodulatory properties (Müller et al., 1993; Janach et al., 2022). IFN- γ attenuates I_h , but unlike type-I IFNs

(Stadler et al., 2014), it leaves pyramidal neurons' excitability unchanged due to acutely augmented inhibition. In particular, IFN- γ augments GABA (γ -amino-butyric acid)ergic currents in the developed rat neocortex (Janach et al., 2020) by increasing synaptic GABA_A channel number in a protein kinase C (PKC)-dependent manner (Janach et al., 2022). In line with this, IFN- γ augments GABAergic currents in the hippocampus (Brask et al., 2004; Flood et al., 2019).

Such alterations of electrical properties could particularly affect neuronal development that is tightly regulated by early neuronal activity in addition to genetic fate (Kirischuk et al., 2017). With regard to the latter, GABA (in particular) plays a key role (Le Magueresse and Monyer, 2013). For instance, on the one hand, GABA acts excitatory during early neurodevelopment due to elevated intracellular chloride (Ben-Ari, 2002), and during development (excitatory) GABA regulates glutamatergic synapse formation *via* N-methyl-D-aspartate receptor (NMDA) activation (Wang and Kriegstein, 2008). On the other hand, GABA may also inhibit neocortical neurons in the first postnatal week (Daw et al., 2007). However, GABAergic neurons also coordinate the development of local cortical networks during a narrow critical postnatal period (Modol et al., 2020). Given these few selected examples of findings concerning the established role of GABA in neuronal development, it does not come as a surprise that the disruption of developing GABAergic neocortical inhibitory network has been implicated in neurodevelopmental disorders, including schizophrenia (Lewis et al., 2005), epilepsy (Cobos et al., 2005), and autism (Pizzarelli and Cherubini, 2011). If IFN- γ altered GABAergic transmission in the developing brain, then this would have broad neurodevelopmental implications, including modulation of cortical maturation.

Taken together, it is clear that the developing brain is vulnerable to disruption of GABAergic transmission, IFN- γ can alter GABAergic currents, and IFN- γ is present at a baseline level or might be elevated by several conditions in the developing brain. Unraveling interactions of the immune system and developing neuronal circuits will foster a better understanding of the biology behind neurodevelopmental diseases. In the long run, such understanding might enable the treatment or even prevention of neurodevelopmental diseases. As a first step, we have here addressed on both, a single cell and a

network level, whether IFN- γ affects inhibitory transmission in neocortical neuronal development, and if so whether the effect is comparable to the one we have previously observed in more mature animals. We have focused on GABAergic synapses at a critical developmental stage (P6–7) during ongoing GABAergic synaptogenesis in rats (Luhmann and Prince, 1991). We mainly investigated spontaneous events because they play a crucial role in synaptic structure and function and act autonomously in regulating synaptic plasticity and homeostasis (Kavalali, 2015).

Materials and methods

Interferon- γ

Chinese hamster ovary or *E. coli*-derived recombinant IFN- γ (U-Cytech, Utrecht, Netherlands; Active Bioscience, Hamburg, Germany) was reconstituted in double distilled water, aliquoted to 1.0 e⁵ IU, and stored at –20°C. Aliquots were thawed directly prior to usage. Final concentration for all experiments was 1,000 IU ml^{–1}.

Animals

For all experiments, Wistar pups of either sex were used on postnatal days 6 and 7 (P6–7). All experiments were carried out in agreement with the European Communities Council Directive of 22 September 2010 (2010/63/EU) under the licenses T 0212/14, T-CH 0034/20 for wild-type rats, and T0215/11 for transgenic rats. For some experiments, we used W-Tg(Slc32a1-YFP*)1Yyan vesicular GABA transporter (VGAT)-Venus transgenic rats that express the yellow fluorescent protein Venus in VGAT expressing neurons, developed by Uematsu et al. (2008) that enabled us to identify interneurons in the slice.

Acute slice preparation

As generally described in Zaqout et al. (2019), decapitation was followed by rapid removal of the brain, which then was transferred into carbogenated (95% O₂; 5% CO₂) 2°C sucrose artificial cerebrospinal fluid (sACSF) containing (in mM): 85 NaCl, 2.5 KCl, 1 NaH₂PO₄, 7 MgCl₂, 26 NaHCO₃, 50 sucrose, 10 D(+)-glucose (Carl Roth, Karlsruhe, Germany), and 0.5 CaCl₂ (Merck, Darmstadt, Germany). 300 μ M thick coronary slice containing somatosensory cortex were cut using a VT1200S vibratome (Leica, Wetzlar, Germany). Slices were recovered for 30 min in 34°C sACSF and were subsequently held at room temperature in modified ACSF containing (in mM): 92 NaCl, 2.5 KCl, 1.2 NaH₂PO₄, 30 NaHCO₃, 25 D(+)-glucose (Carl Roth), 5 sodium ascorbate, 20 2-[4-(2-hydroxyethyl)piperazin-1-yl]ethanesulfonic acid (HEPES), 3 sodium pyruvate, 2 MgSO₄,

2 CaCl₂ (Merck), and 2 thiourea (VWR Chemicals, Radnor, PA, United States) until recording. All variations of ACSF were continuously carbogenated.

Ex vivo patch clamp recordings

Slices were transferred to a submerged type recording chamber continuously perfused with carbogenated ACSF containing (in mM): 119 NaCl, 2.5 KCl, 1 NaH₂PO₄, 1.3 MgCl₂, 26 NaHCO₃, 10 D(+)-glucose (Carl Roth), and 2.5 CaCl₂ (Merck) at 32 \pm 2°C. Slices were visualized using infrared differential interference contrast (DIC) microscopy with a Zeiss Axioskop 2 FS plus (Carl Zeiss, Oberkochen, Germany). Glass micropipettes (2–5 M Ω) were pulled from lead (PG10165-4, WPI, Sarasota, FL, United States) or borosilicate (GB150-10P, Science Products, Hofheim, Germany) glass capillaries using a P-97 micropipette puller (Sutter Instrument, Novato, CA, United States). For IPSC recordings, 6-cyano-7-nitroquinoxaline-2,3-dione (CNQX, 20 μ M) and D(-)-2-Amino-5-phosphonopentanoic acid (DAP-5, 25 μ M) (Tocris, Bristol, United Kingdom) were added to the perfusate to block glutamatergic ion currents and pipettes were filled with a high chloride internal solution containing (in mM): 140 CsCl (Biomol, Hamburg, Germany), 4 NaCl, 1 MgCl₂ (Carl Roth), 10 HEPES, 0.1 ethylene glycol-bis(β -aminoethyl ether)-N,N,N',N'-tetraacetic acid (EGTA), 0.3 GTP, 2 Mg²⁺-ATP (Merck), (305 mOsm, pH set to 7.25 with KOH), and 5 mM QX-314 (Merck) to improve the signal-to-noise ratio. Calphostin C (Enzo Life Sciences, NY, United States) was dissolved in DMSO at 1 mM and aliquoted to working sizes. Prior to respective experiments, Calphostin C was added to the pipette solution to a final concentration of 100 nM. When Calphostin C was used, slice and pipette were continuously exposed to full-spectrum white light (Bruns et al., 1991). Other drugs in this study included: Bicuculline methiodide (Tocris), S-Nitroso-N-acetylpenicillamine (SNAP) (cayman chemical, Ann Arbor, MI, United States), 1H-[1,2,4]oxadiazolo[4,3-a]quinoxalin-1-one (ODQ) (Tocris), tetrodotoxin (TTX) (Tocris), and N-[3(Aminomethyl)benzyl] acetamidine dihydrochloride (1400W) (Sigma-Aldrich, St. Louis, United States). ODQ was dissolved in dimethylsulfoxide (DMSO) at 100 mM and aliquoted to working sizes. Total DMSO in perfusate never exceeded 0.1%. All other reagents and drugs, unless specified otherwise, were dissolved and aliquoted in double distilled water.

For current-clamp recordings, internal solution contained (in mM) 120 K-Gluconate, 11 EGTA, 10 HEPES, 10 phosphocreatine, 1 MgCl₂, 2 Mg²⁺-ATP, 0.3 GTP, 10 KCl (Merck), and 1 CaCl₂ (Carl Roth). After establishing whole-cell configuration, pipette solution was allowed to diffuse into the cell, and blockers were bath applied for at least 5 min before recording started. Spontaneous/minature inhibitory

postsynaptic current (s/mIPSC) recordings were excluded from analysis when series resistance (R_s) changed by more than 25%, initial IPSC frequency was below $10 \text{ events min}^{-1}$ ($0.167 \text{ events s}^{-1}$), holding current (that was mainly due Cl^- enhanced tonic inhibition and Cs^+ mediated depolarization, **Supplementary Figure 1A**) changed abruptly or hyperpolarized beyond -800 pA , indicating the development of technical leak. If access resistance changed during experiments, efforts were made to reestablish access, and experiments were discontinued if unsuccessful. IFN- γ exposure time was aimed at 25 min. In some cases, a later time point (up to 30 min) or an earlier time point (minimum 15 min) was used. Reasons included changed series resistance that had to be corrected or sudden changes in holding current. An overview of exposure times is given in **Supplementary Figure 1B**, population data averages are stated in the respective figure legends. Electric activity was recorded using an EPC-10 double amplifier (HEKA Elektronik GmbH, Reutlingen, Germany), digitized at 6.25 kHz after Bessel filtering (2.5 kHz), and stored *via* PatchMaster 2.91 (HEKA). Spontaneous and miniature IPSCs were analyzed using Synaptosoft MiniAnalysis Software (Synaptosoft Inc., Fort Lee, NJ, United States). Negative deflections deviating from baseline by more than 3 RMS (root mean square) noise were counted as IPSCs. Upon manual review, erroneously detected events were removed and missed events were added. For every data point, events from two consecutive minutes of recordings were averaged. For washout experiments, slices were incubated in ACSF containing IFN- γ , CNQX ($20 \text{ }\mu\text{M}$), and DAP-5 ($25 \text{ }\mu\text{M}$) at 34°C for 30 min. IPSCs were recorded under continuous perfusion of the same solution until stable recording conditions were achieved. Then, IFN- γ was removed from the perfusion. Electrically evoked orthodromic IPSCs have been rarely demonstrated before P14 (Luhmann and Prince, 1991). In this study, stimulating currents ($0.02\text{--}1 \text{ mA}$, applied for $100 \text{ }\mu\text{s}$, delivered through a $1 \text{ M}\Omega$ glass electrode filled with ACSF, positioned $150 \text{ }\mu\text{m}$ apically and $200 \text{ }\mu\text{m}$ laterally of the recorded neuron) reliably evoked delayed inward current responses that could be blocked by bicuculline, confirming their GABAergic identity (**Supplementary Figure 2E**). To avoid stimulus-induced long-term changes in synaptic transmission, paired stimuli were applied at 10 s intervals. For paired-pulse experiments, R_s changes up to 35% were tolerated. Paired-pulse recordings were analyzed using FitMaster v2 \times 90.5 (HEKA). For every datapoint, 20 traces were analyzed by dividing the amplitude of the second-evoked IPSC through the amplitude of the first. Of 20 ratios, the mean ratio was calculated for comparison. Current-clamp recordings were analyzed using FitMaster software for spike detection and counting. Calculations requiring polynomial fitting were performed using OriginPro 2022 (OriginLab, Northampton, MA, United States). Neurons recorded in voltage clamp had a mean capacitance of $C_{\text{before}} = 118.0 \pm 3.4 \text{ pF}$ that slightly decreased to $C_{\text{after}} = 112.0 \pm 3.2 \text{ pF}$ ($p < 0.0001$, $n = 111$, $N = 42$ paired t -test) over the course of voltage clamp recordings.

Post hoc visualization

For cell selection, pyramidal neurons were identified by their typical morphology in DIC microscopy, VGAT expressing interneurons could be identified *via* fluorescence. To validate correct cell selection, in a subset of recordings, N_e -(+)-Biotinyl-L-lysine (biotin) (Invitrogen, Waltham, MA, United States) was added to the pipette solution to a final concentration of 1%. After recording, slices were fixed in cold phosphate-buffered saline with 4% paraformaldehyde for 1 h. Then, slices were washed in 0.1 M phosphate buffer and subsequently incubated in 4°C phosphate buffer with 0.3% Triton-X (Sigma-Aldrich), 0.05% NaN_3 (Merck), and fluorescent-conjugated streptavidin (Alexa Fluor 647, 1:1,000, Invitrogen) for 48 h. Following another washing step, slices were mounted and imaged using a laser scanning confocal microscope (FV1000, Olympus, Tokyo, Japan).

Multielectrode array recordings

Neuronal activity was recorded with a Multielectrode Array (MEA), consisting of 60 electrodes in an 8×8 layout with electrode diameters of $10 \text{ }\mu\text{m}$, and $200 \text{ }\mu\text{m}$ spacing (60MEA200/10iR, Multi Channel Systems (MCS), Reutlingen, Germany). Slices, prepared as described above, were placed in the recording chamber, so that somatosensory cortex covered the electrodes. The recording chamber was briefly drained to ensure contact between slice surface and electrodes. Slices were secured by steel anchors (Warner Instruments, Holliston, United States) and were continually perfused with carbogenated ACSF ($4\text{--}6 \text{ ml min}^{-1}$), maintained at 30°C by the Pt100 Temperature Controller System (MCS). In all recordings, the K^+ -channel blocker 4-Aminopyridine ($50 \text{ }\mu\text{M}$, 4-AP, Sigma-Aldrich) was used to enhance activity. Recordings were started after 5 min of stabilization and lasted 30 min, under control and test condition, respectively. Electrical activity was recorded by the MEA 2100-120 system (bandwidth = $1\text{--}3,000 \text{ Hz}$, gain = $\times 10$, MCS) and sampled at 10 kHz using Multi Channel Experimenter software (MCS). Given the electrode distance of $200 \text{ }\mu\text{m}$, it is unlikely but possible that events cross the detection threshold on multiple channels. Event sorting was performed with the spyKing circus algorithm (Yger et al., 2018) to avoid repetitive counting. Event detection threshold was set to 8 MAD (mean absolute deviation) from baseline of a given channel. Data were high-pass filtered at 300 Hz (3rd-order Butterworth filter) and whitened using the spyKing circus software.¹ Event sorting was performed over the entire recording, including control and test conditions. Sorted data were reviewed with PHY graphical user interface.² For further analysis, we included the

¹ <https://github.com/spyking-circus/spyking-circus>

² <https://github.com/cortex-lab/phy>

last 20 min of each condition. Only event clusters with normally distributed amplitudes were considered for analysis.

Statistical analysis and data reporting

The study was designed to enable longitudinal pairwise comparison. Note that a direct comparison of IPSC frequencies between different neurons is hampered by the huge variance of the frequency of GABAergic inputs at this developmental stage that might be due to staggered maturation, and many other factors (for instance slicing angle, depth in the slice, quality of individual preparation, **Supplementary Figures 2A–C**). All statistical analyses were performed using OriginPro 2022 (OriginLab). Datasets were tested for normal distribution using the Shapiro–Wilk test. In case of rejection ($p \leq 0.05$), the Wilcoxon signed-rank test for paired data was used to test for statistical significance. Probability distributions were tested for equality using the Kolmogorov–Smirnov test. Due to low event counts, data for all recordings under a certain experimental condition were pooled for probability distributions. Total number of events analyzed, number of recordings, and number of animals are given in the respective figure legends. When normal distribution could not be rejected, Student's *t*-test or paired Student's *t*-test was used, respectively. The null hypothesis was rejected for $p \leq 0.05$. All data are given in $d_{\text{variable}} = \text{mean} \pm \text{standard error of the mean}$ (P , statistical test, n = number of recordings, N = number of animals), unless otherwise specified.

Figures and images

Figures were plotted using OriginPro 2022 (OriginLab). Images of biocytin-filled neurons were adjusted (brightness inversion, contrast, scale bars, z-stack projection) with Fiji software (Schindelin et al., 2012). Final assembly was achieved using Corel Draw 2017 (Corel Corporation, Ottawa, ON, Canada).

Results

Interferon- γ acutely increased sIPSC frequency and amplitude

We have previously found an increased inhibition in the neocortex of late juvenile and adult rats under the influence of IFN- γ (Janach et al., 2020). Given the prominent role of GABAergic transmission in cortical development, herein, we have studied IFN- γ effects on developing neurons. In detail, we whole-cell recorded spontaneous inhibitory postsynaptic currents (sIPSCs) in somatosensory pyramidal layer 5 neurons

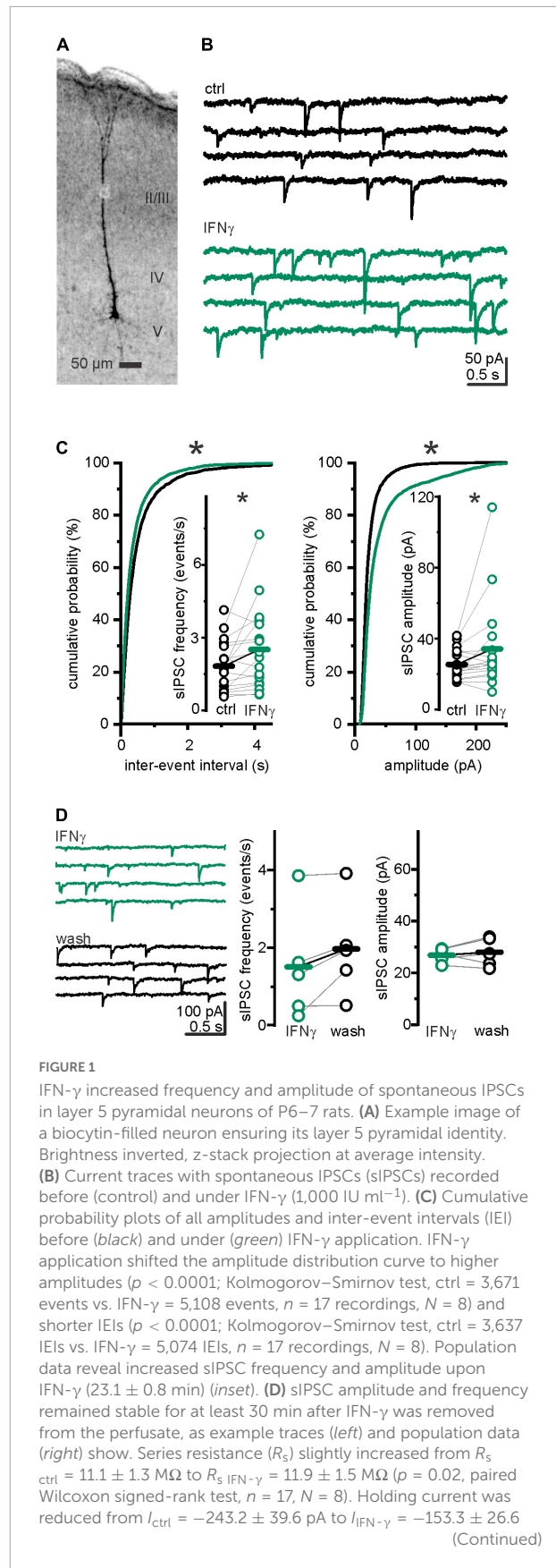


FIGURE 1

pA ($p = 0.02$, paired Wilcoxon signed-rank test, $n = 17$, $N = 8$). Elevated R_s cannot cause IPSC amplitude or frequency increase. During washout experiments, series resistance slightly increased from $R_{s \text{ IFN-}\gamma} = 14.6 \pm 2.1 \text{ M}\Omega$ to $R_{s \text{ wash}} = 16.4 \pm 2.4 \text{ M}\Omega$ ($p = 0.04$, paired t -test, $n = 5$, $N = 1$). Holding current remained comparable ($I_{\text{hold IFN-}\gamma} = -144.0 \pm 26.1 \text{ pA}$ vs. $I_{\text{hold wash}} = -121.9 \pm 20.0 \text{ pA}$; $p = 0.3$, paired t -test, $n = 5$, $N = 1$). * $p < 0.05$.

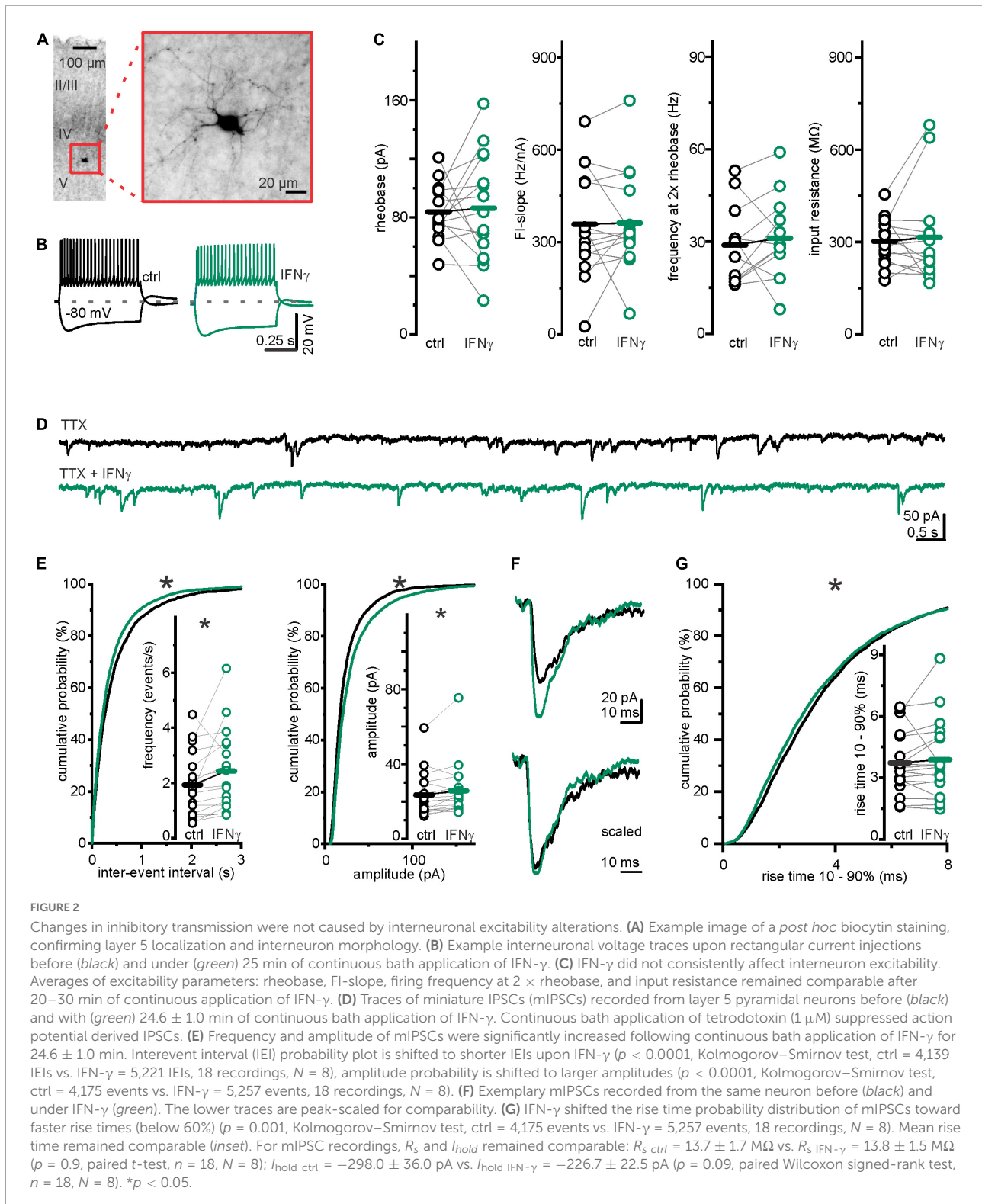
(Figure 1A) from P6 to 7 Wistar rats. As seen in more mature neurons, bath-applied IFN- γ (1,000 IU ml $^{-1}$) increased the mean amplitude of sIPSCs at P6–7 from $I_{\text{ctrl}} = 25.6 \pm 2.2 \text{ pA}$ to $I_{\text{IFN-}\gamma} = 36.1 \pm 6.7 \text{ pA}$ ($p = 0.005$, Wilcoxon signed-rank test, $n = 17$, $N = 8$; Figures 1B,C). Surprisingly, the sIPSC frequency also increased markedly from $f_{\text{ctrl}} = 1.96 \pm 0.27 \text{ events s}^{-1}$ to $f_{\text{IFN-}\gamma} = 2.73 \pm 0.46 \text{ events s}^{-1}$ ($p = 0.039$, Wilcoxon signed-rank test, $n = 17$, $N = 8$). We then addressed whether these relatively acute effects ceased upon removal of IFN- γ . We found that, when preincubated with IFN- γ for at least 30 min, sIPSC frequency and amplitude remained stable for at least 30 min during washout ($f_{\text{IFN-}\gamma} = 1.51 \pm 0.64 \text{ events s}^{-1}$ vs. $f_{\text{wash}} = 1.97 \pm 0.56 \text{ events s}^{-1}$, $p = 0.09$, paired t -test, $n = 5$, $N = 1$; $I_{\text{IFN-}\gamma} = 26.8 \pm 1.2 \text{ pA}$ vs. $I_{\text{wash}} = 28.0 \pm 2.5 \text{ pA}$, $p = 0.5$, paired t -test, $n = 5$, $N = 1$; Figure 1D). This indicates that IFN- γ induced changes in GABAergic transmission do not vanish within 30 min. Instead, the trend toward higher frequencies plausibly indicates an inductive effect of IFN- γ on sIPSC frequency. To test whether our intracellular solution produced changes in sIPSC frequency or amplitude during long-term experiments (i.e., if this is merely a time-dependent effect), we recorded sIPSCs for 15–20 min in plain ACSF and found that both, frequency ($f_{\text{before}} = 2.4 \pm 0.3 \text{ events s}^{-1}$ vs. $f_{\text{after}} = 2.5 \pm 0.4 \text{ events s}^{-1}$; $p = 0.62$, paired t -test, $n = 11$, $N = 3$) and amplitude ($I_{\text{before}} = 27.5 \pm 3.1 \text{ pA}$ vs. $I_{\text{after}} = 24.3 \pm 2.2 \text{ pA}$; $p = 0.19$, paired t -test, $n = 11$, $N = 3$), remained comparable (Supplementary Figure 1C). The considerable increase in sIPSC frequency may suggest a presynaptic action in addition to the previously described postsynaptic mechanism (Janach et al., 2022) behind the increased amplitude. Therewith, the observed augmentation of inhibition by IFN- γ is not only reproduced in the developing rat brain but exhibits a feature that is not consistently observed at later stages of brain development.

Interferon- γ left interneuron excitability unchanged and increased inhibitory postsynaptic currents frequency under voltage-dependent sodium channel blockage

One possible presynaptic mechanism underlying the observed IFN- γ -induced increase in sIPSC frequency in

early postnatal development includes augmented interneuron excitability. As medial ganglionic eminence and preoptic area interneurons have completed migration by the end of the first postnatal week (Bortone and Polleux, 2009), we performed current-clamp recordings in layer 5 interneurons that we identified by VGAT-Venus expression. For *post hoc* verification, we filled the neurons with biocytin and visualized them following the recording (Figure 2A). Bath applied IFN- γ left averaged parameters for sub- and suprathreshold excitability comparable, including: Input resistance, determining voltage change upon current injection, $R_{\text{in ctrl}} = 302.0 \pm 19.5 \text{ M}\Omega$ vs. $R_{\text{in IFN-}\gamma} = 315.2 \pm 39.2 \text{ M}\Omega$, ($p = 0.67$, paired t -test, $n = 15$, $N = 7$), rheobase, lowest current capable of eliciting a single action potential, $I_{\text{rheobase ctrl}} = 83.7 \pm 4.9 \text{ pA}$ vs. $I_{\text{rheobase IFN-}\gamma} = 86.3 \pm 9.7 \text{ pA}$ ($p = 0.79$, paired t -test, $n = 15$, $N = 7$), slope of the frequency-current relationship $FI\text{-slope}_{\text{ctrl}} = 358.0 \pm 44.5 \text{ Hz nA}^{-1}$ vs. $FI\text{-slope}_{\text{IFN-}\gamma} = 362.2 \pm 40.9 \text{ Hz nA}^{-1}$ ($p = 0.9$, paired t -test, $n = 15$, $N = 7$) and frequency at $2 \times$ rheobase $f_{2 \times \text{RB ctrl}} = 28.8 \pm 3.7 \text{ Hz}$ vs. $f_{2 \times \text{RB IFN-}\gamma} = 31.1 \pm 4.0 \text{ Hz}$ ($p = 0.5$, paired t -test, $n = 12$, $N = 5$). Notably, FI-slope and firing frequency at $2 \times$ rheobase are parameters that reflect a neuron's input-output relationship (Figures 2B,C).

Given the high variability and axonal divergence of GABAergic interneurons, we could not exclude subtype-specific IFN- γ action on interneuron excitability. We therefore next investigated whether the observed effect is dependent on presynaptic firing. Because IPSCs that might be elicited by presynaptic action potentials were not distinguishable from those resulting from spontaneous vesicle release by amplitude (Supplementary Figure 1D), we investigated the spontaneous vesicle release separately. We recorded miniature IPSCs (mIPSCs) from layer 5 pyramidal neurons in the presence of tetrodotoxin (TTX, 1 μM), a blocker of voltage-gated sodium channels. Despite continuously suppressed interneuronal firing, upon IFN- γ application mIPSC frequency increased from $f_{\text{ctrl}} = 1.93 \pm 0.27 \text{ events s}^{-1}$ to $f_{\text{IFN-}\gamma} = 2.43 \pm 0.34 \text{ events s}^{-1}$ ($p = 0.04$, paired t -test, $n = 18$, $N = 8$) and amplitude increased from $I_{\text{ctrl}} = 23.5 \pm 2.8 \text{ pA}$ to $I_{\text{IFN-}\gamma} = 25.7 \pm 3.4 \text{ pA}$ ($p = 0.03$, Wilcoxon signed-rank test, $n = 18$, $N = 8$) (Figures 2D,E). It remained possible that synapses of distinct interneuron groups (that connect to different parts of the neuron) are differentially affected by IFN- γ . Because the kinetics of synaptic currents, in particular the rise time (Xiang et al., 2002), give insights on synapse localization along the somatodendritic axis (e.g., perisomatic vs. dendritic site), we analyzed 10–90% rise times of mIPSCs before and after IFN- γ application and found that the mean rise time remained similar (rise time $_{\text{ctrl}} = 3.7 \pm 0.4 \text{ ms}$ vs. rise time $_{\text{IFN-}\gamma} = 3.9 \pm 0.4 \text{ ms}$, $p = 0.5$, paired t -test, $n = 18$, $N = 8$). However, the cumulative probability distribution reveals a slight shift toward shorter rise times (Figures 2F,G). Because of the small yet significant difference between the probability distributions, we are not confident that this can



be interpreted solely as an increased portion of perisomatic inhibition upon IFN- γ addition. A better distinction/a greater gap might be stashed by the relative electrotonic compactness of developing neurons.

Taken together, we have found that the IFN- γ -induced increase in sIPSC frequency appears independent of and cannot be attributed to an increase in layer 5 interneuron excitability or presynaptic firing.

Protein kinase C inhibitor calphostin C, applied to the postsynaptic neuron, prevented interferon- γ mediated increase in mIPSC amplitude, but not frequency

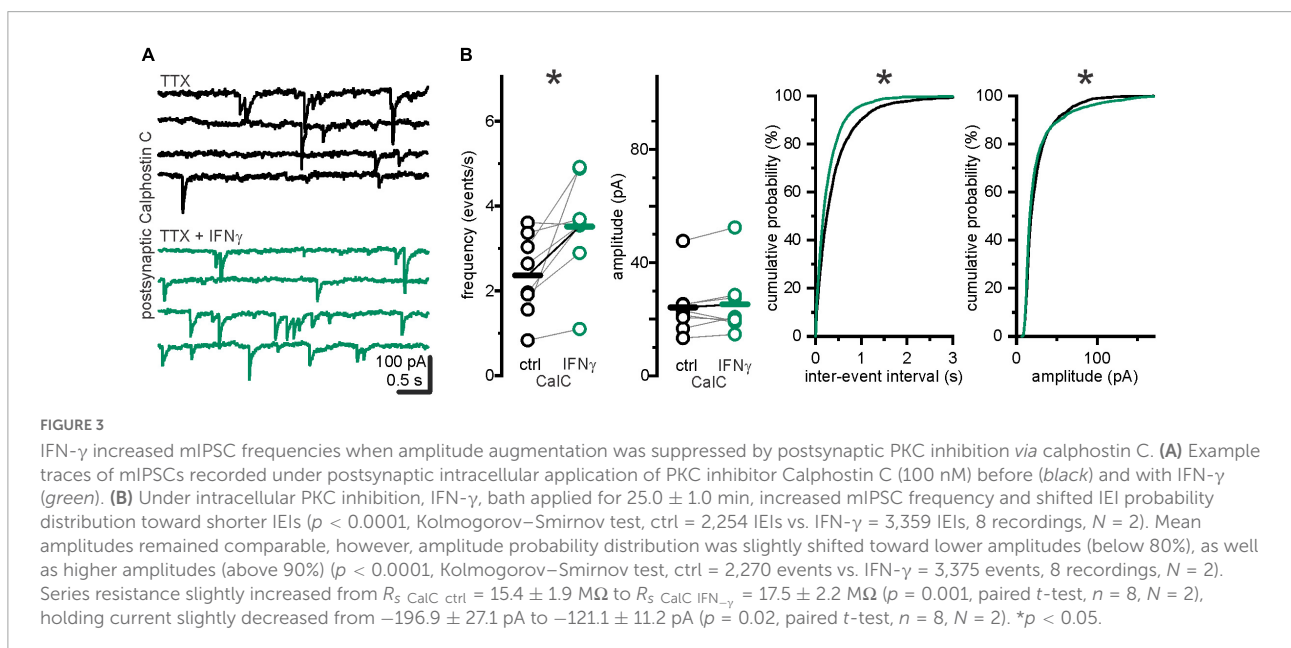
We have previously reported that IFN- γ augments GABAergic currents by promoting postsynaptic membrane association of GABA_A receptors *via* a PKC-dependent mechanism (Janach et al., 2022) in late juvenile rats. To test whether the observed increase in s/mIPSC frequency is caused by higher amplitudes (i.e., whether more amplitudes are elevated above baseline noise levels), we recorded mIPSCs under postsynaptic block of PKC by Calphostin C (100 nM). Calphostin C in the postsynaptic neuron prevented an increase in mIPSC amplitude upon IFN- γ application ($I_{\text{CalC}}^{\text{ctrl}} = 24.1 \pm 3.7$ pA vs. $I_{\text{CalC}}^{\text{IFN-}\gamma} = 25.3 \pm 4.2$, $p = 0.4$, Wilcoxon signed-rank test, $n = 8$, $N = 2$, Figure 3). However, mIPSC frequency increased from $f_{\text{CalC}}^{\text{ctrl}} = 2.36 \pm 0.3$ events s^{-1} to $f_{\text{CalC}}^{\text{IFN-}\gamma} = 3.52 \pm 0.42$ events s^{-1} ($p = 0.02$, paired t -test, $n = 8$, $N = 2$).

These findings suggest that the observed IFN- γ -induced IPSC amplitude increase at the end of the first postnatal week is both postsynaptic and PKC mediated, as previously described for older stages (Janach et al., 2022). In addition, they indicate separate mechanisms for IPSC amplitude and frequency increase upon IFN- γ application. Thus, the persistence of the IFN- γ -induced increase in frequency under block of the major known postsynaptic mediator renders a postsynaptic contribution to the frequency effect unlikely.

The interferon- γ -induced increase in sIPSC frequency was mimicked by nitric oxide and depended on inducible nitric oxide synthase and soluble guanylate cyclase

IFN- γ induces nitric oxide (NO) production (Blanchette et al., 2003). NO is also a known regulator of synaptic release (reviewed in Hardingham et al., 2013): NO donors increase (Li et al., 2004; Yang and Cox, 2007) and knockout of NO receptor soluble guanylate cyclase (sGC) decreases IPSC frequencies (Wang et al., 2017). Therefore, the IFN- γ induced elevation of IPSC frequency we observed in pyramidal neurons at P6–7 might be caused by elevated NO levels. Decreased IPSC frequencies upon NO, however, have been reported (Lee, 2009).

To test whether NO is sufficient to induce an increase in inhibitory release at P6–7, we recorded sIPSCs and added SNAP (300 μM), an NO releasing agent widely used to study the impact of NO on neurophysiology (Li et al., 2004). Within 5 min, sIPSC frequency increased from $f_{\text{ctrl}} = 2.79 \pm 0.36$ events s^{-1} to $f_{\text{SNAP}} = 3.32 \pm 0.43$ events s^{-1} ($p = 0.002$, paired t -test, $n = 11$, $N = 3$), while sIPSC amplitude remained comparable ($I_{\text{ctrl}} = 24.0 \pm 2.8$ vs. $I_{\text{SNAP}} = 22.2 \pm 1.6$ pA; $p = 0.5$, Wilcoxon signed-rank test, $n = 11$, $N = 3$; Figure 4A). NO donors can activate leaky, Cs⁺ sensitive, K⁺-channels (Kang et al., 2007). In our experiments, however, the Cs⁺ containing pipette solution should omit putative K⁺ currents. Accordingly, holding currents remained similar upon SNAP application: $I_{\text{hold}}^{\text{ctrl}} = -265.8 \pm 44.3$ pA vs. $I_{\text{hold}}^{\text{SNAP}} = -262.9 \pm 45.9$ pA ($p = 0.73$, paired t -test, $n = 11$, $N = 3$).



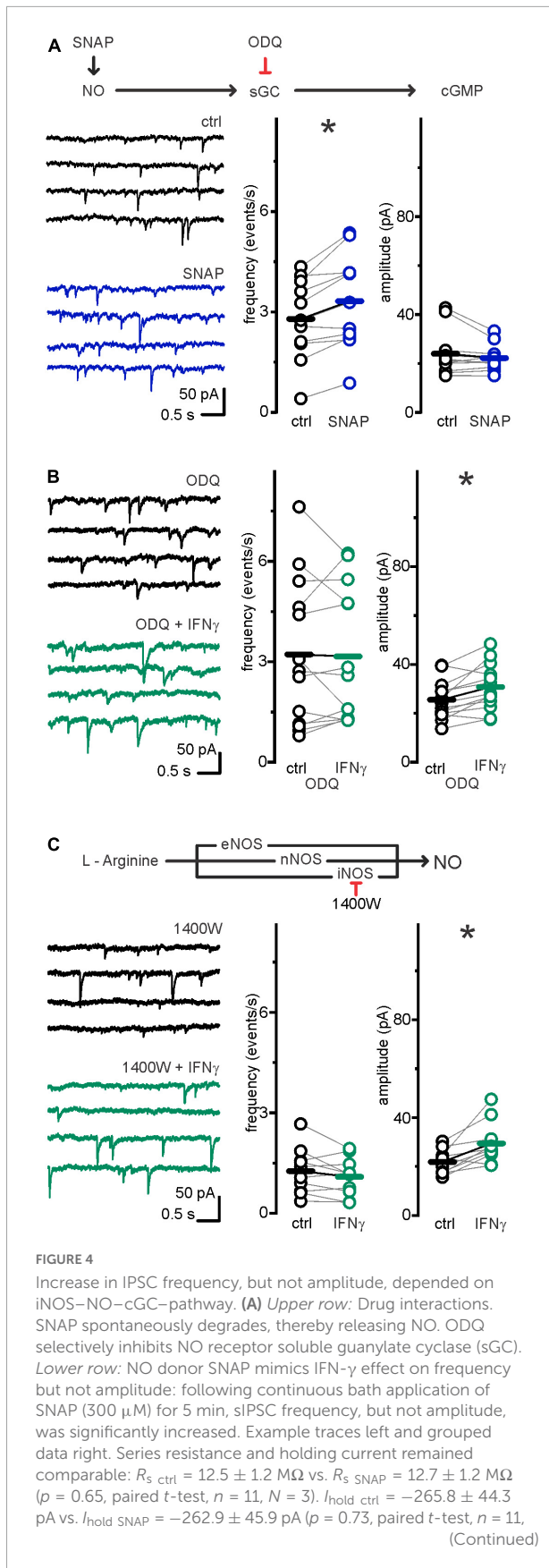


FIGURE 4

$N = 3$). **(B)** sGC inhibitor ODQ (100 μ M) inhibited sIPSC frequency, but not amplitude increase upon IFN- γ , bath applied for 23.1 ± 1.1 min. Example current traces left, grouped data right. Series resistance and holding current remained comparable: R_s ODQ ctrl = 12.1 ± 1.8 M Ω vs. R_s ODQ IFN- γ = 11.8 ± 1.5 M Ω ($p = 0.6$, paired t -test, $n = 13$, $N = 7$). I_{hold} ODQ ctrl = -365.8 ± 45.1 pA vs. I_{hold} ODQ IFN- γ = -306.3 ± 33.5 pA ($p = 0.1$, paired t -test, $n = 13$, $N = 7$). **(C)** NO is produced by three isoforms of nitric oxide synthase [inducible (iNOS), neuronal (nNOS), and endothelial (eNOS)]. In the presence of iNOS inhibitor 1400W (10 μ M), IFN- γ , bath applied for 22.1 ± 0.8 min, increased sIPSC amplitude, but not frequency. Example current traces left, grouped data right. Series resistance and holding current remained comparable: R_s 1400W ctrl = 14 ± 1.7 M Ω vs. R_s 1400W IFN- γ = 13.6 ± 1.6 M Ω ($p = 0.66$, paired t -test, $n = 10$, $N = 4$). I_{hold} 1400W ctrl = -319.9 ± 34.6 pA vs. I_{hold} 1400W IFN- γ = -308.4 ± 43.6 pA ($p = 0.13$, paired t -test, $n = 10$, $N = 4$). * $p < 0.05$.

NO has been shown to impact GABAergic synaptic release *via* binding to its direct receptor sGC (Wang et al., 2017), and sGC is expressed in layer 5 neurons around P6–7 (Ding et al., 2005). If IFN- γ effects on presynaptic release are NO-mediated, blocking sGC should abolish them. Therefore, we tested this by utilizing ODQ (100 μ M), a selective sGC blocker (Yang and Cox, 2007; Wang et al., 2017). Indeed, IFN- γ application failed to increase the sIPSC frequency in the presence of ODQ ($f_{\text{ODQ ctrl}} = 3.22 \pm 0.61$ vs. $f_{\text{ODQ IFN-}\gamma} = 3.16 \pm 0.56$ events s^{-1} ; $p = 0.67$, Wilcoxon signed-rank test, $n = 13$, $N = 7$). The IFN- γ induced increase in sIPSC amplitudes from $I_{\text{ODQ ctrl}} = 25.5 \pm 2.2$ to $I_{\text{ODQ IFN-}\gamma} = 30.8 \pm 2.6$ pA ($p = 0.005$, paired sample t -test, $n = 13$, $N = 7$), however, persisted under ODQ application (Figure 4B). This suggests that NO binding to sGC specifically mediates the increase in sIPSC frequency.

IFN- γ may induce NO production *via* inducible nitric oxide synthase (iNOS) (Stuehr and Marletta, 1987). To assess whether iNOS is involved in presynaptic IFN- γ effects, we recorded sIPSCs in neocortical pyramidal neurons in the presence of the potent and irreversible iNOS inhibitor 1400W (Garvey et al., 1997). We observed that the addition of 1400W (10 μ M) reliably prevented sIPSC frequency increase upon IFN- γ application: Under 1400W, IFN- γ increased sIPSC amplitude ($I_{1400W \text{ ctrl}} = 21.8 \pm 1.6$ to $I_{1400W \text{ IFN-}\gamma} = 29.4 \pm 2.7$ pA; $p = 0.007$, paired t -test, $n = 10$, $N = 3$), whereas sIPSC frequency remained comparable ($f_{1400W \text{ ctrl}} = 1.26 \pm 0.22$ to $f_{1400W \text{ IFN-}\gamma} = 1.09 \pm 0.18$ events s^{-1} , $p = 0.16$, paired t -test, $n = 10$, $N = 3$; Figure 4C). Of note, although 1400W may partly block neuronal (nNOS) (Garvey et al., 1997) with a nominal IC_{50} of 7.3 μ M (Alderton et al., 2001), concentrations needed to effectively inhibit nNOS are ≥ 100 μ M (Pigott et al., 2013).

In summary, these data indicate that IFN- γ increases presynaptic GABA release in an iNOS and sGC-dependent fashion.

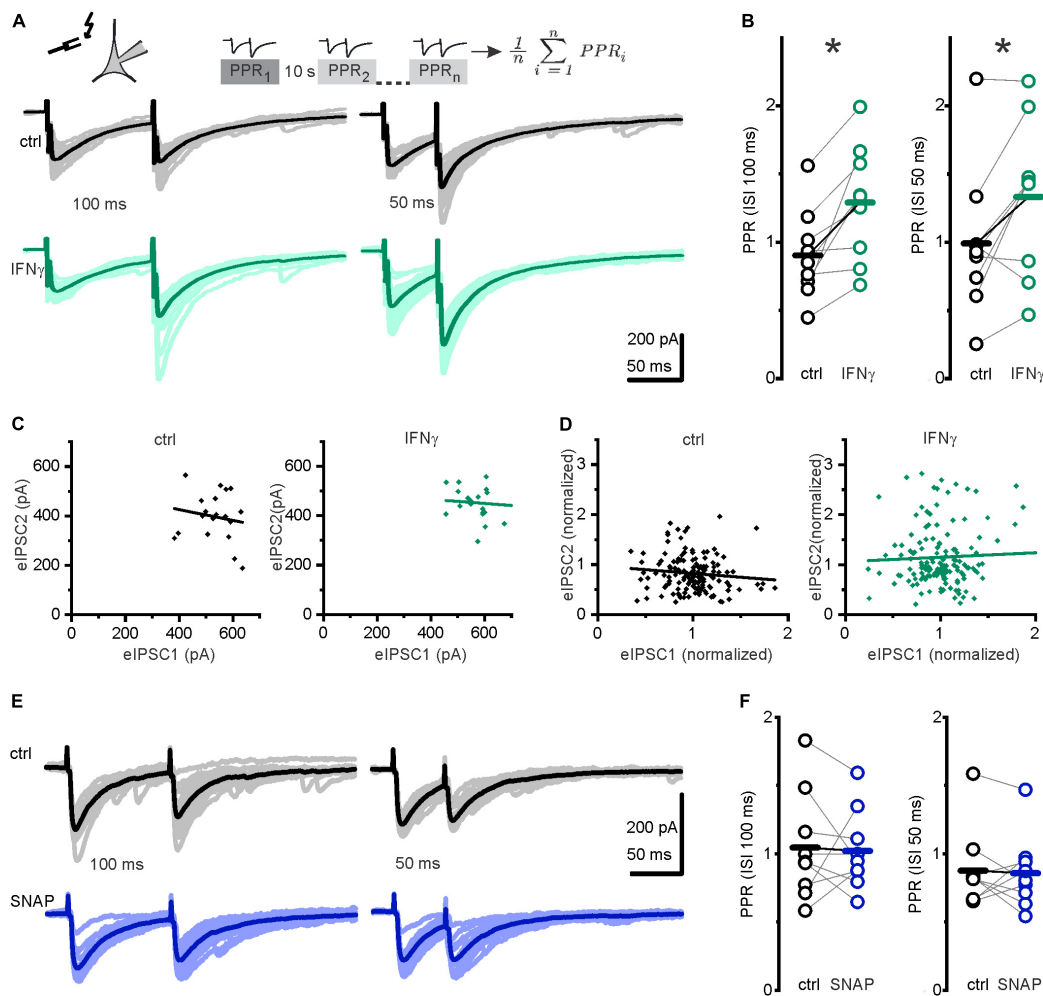


FIGURE 5

IFN- γ promoted paired-pulse facilitation. (A) *Upper row*: Paired-pulse paradigm: two consecutive IPSCs were evoked by electrical stimulation at 100 or 50 ms interstimulus interval (ISI). The paired-pulse ratio (PPR) was calculated by division of the second eIPSC amplitude by the first eIPSC amplitude. Twenty individual paired-pulse ratios were recorded and averaged for every data point. Stimulation was paused for 10 s between each pair. *Lower row*: Pairs of evoked IPSCs at 100 ms ISI (*left*) and 50 ms ISI (*right*), without (*black*) and with IFN- γ (*green*). Darker lines represent averages, stimulus artifacts truncated for clarity. Note comparable kinetics of evoked and spontaneous IPSCs of interfering sIPSCs during eIPSC decay. (B) IFN- γ , bath applied for 20 min, increased PPR (second amplitude divided by first amplitude). (C,D) PPR appears to be independent on previous release. (C) Plot of peak amplitudes of eIPSC2 vs. eIPSC1 for individual paired pulses from one neuron before (*ctrl*, *black*) and under 20 min of IFN- γ (*IFN- γ* , *green*). (D) Plot of normalized amplitude of eIPSC2 against eIPSC1 for all neurons investigated. Amplitudes were normalized to mean value of eIPSC1 for each pair. Lines represent linear regression [correlation coefficient -0.16 ($p = 0.5$) for *ctrl* and -0.08 ($p = 0.7$) for IFN- γ for one neuron (C) and -0.11 ($p = 0.17$) for *ctrl* and 0.04 ($p = 0.6$) for IFN- γ for all neurons (D)]. (E) Example traces of paired-pulse recordings before (*black*) and under (*blue*) application of the NO donor SNAP. Trace averages are shown in strong colors, and individual traces in light colors. (F) Paired-pulse ratios remained comparable after the application of SNAP (300 μ M) for 5 min. Series resistance slightly increased from $R_{s \text{ ctrl}} = 11.1 \pm 0.8 \text{ M}\Omega$ to $R_{s \text{ IFN-}\gamma} = 13.5 \pm 1.0 \text{ M}\Omega$ ($p = 0.01$, paired *t*-test, $n = 9$, $N = 6$). Holding current remained grossly comparable $I_{\text{hold ctrl}} = -316.7 \pm 34.6 \text{ pA}$ vs. $I_{\text{hold IFN-}\gamma} = -252.4 \pm 35.9 \text{ pA}$, $p = 0.06$, paired *t*-test, $n = 9$, $N = 6$). For SNAP experiments, series resistance and holding current remained comparable ($R_{s \text{ ctrl}} = 18.4 \pm 2.5 \text{ M}\Omega$ vs. $R_{s \text{ SNAP}} = 19.8 \pm 2.5 \text{ M}\Omega$, $p = 0.1$, paired *t*-test, $n = 9$, $N = 3$; $I_{\text{hold ctrl}} = -185.7 \pm 36.0 \text{ pA}$ vs. $I_{\text{hold SNAP}} = -127.3 \pm 13.6 \text{ pA}$). * $p < 0.05$.

Interferon- γ facilitated short-term synaptic plasticity in GABAergic presynapses

Spontaneous and evoked GABA release neither completely overlaps nor is entirely separable (Horvath et al., 2020). To differentiate between IFN- γ effects on evoked vs. spontaneous

GABA release, we used a paired-pulse paradigm revealing a paired-pulse ratio (PPR) that is commonly seen as an index of release probability (Kravchenko et al., 2006). We recorded eIPSCs evoked by pairs of stimuli at interstimulus intervals (ISI) of 100 or 50 ms. IFN- γ , bath applied for 20 min, consistently increased the PPR (defined as amplitude of the second response divided by the amplitude of the first

response) at both intervals tested (from $PPR100ms_{ctrl} = 0.9 \pm 0.1$ to $PPR100ms_{IFN-\gamma} = 1.3 \pm 0.1$, $p = 0.005$, paired t -test, $n = 9$, $N = 6$ and from $PPR50ms_{ctrl} = 1.0 \pm 0.2$ to $PPR50ms_{IFN-\gamma} = 1.3 \pm 0.2$, $p = 0.02$, paired t -test, $n = 9$, $N = 6$; **Figures 5A,B**), i.e., it shifted the PPR toward facilitation. To estimate whether the PPR depends on the initial eIPSC amplitude, we used linear regression analysis in plots of second eIPSC amplitude vs. first eIPSC amplitude. Under control conditions, correlation coefficients (Pearson's r) ranged from -0.6 to 0.1 , none of these were statistically significant. Under IFN- γ application, correlation coefficients ranged from -0.67 to 0.45 , one point of which was statistically significant at $r = -0.46$, $p = 0.04$. Using normalized amplitudes, we then pooled all experiments in each group. Pooled analysis showed no correlation between first and second eIPSC amplitudes ($r_{ctrl} = -0.11$, $p = 0.17$; $r_{IFN-\gamma} = 0.04$, $p = 0.6$, **Figures 5C,D**). This implies that PPR under control conditions and under the influence of IFN- γ does not depend on previous release as is seen in more mature rat neocortical pyramidal neurons (**Supplementary Figures 2E,G**; Xiang et al., 2002).

Because we have here investigated short-term plasticity (i.e., the ratio of consecutive eIPSC amplitudes at a given time point), we slightly relaxed the restrictions on R_s for this particular series (see section "Materials and methods"). Subsequently, only four recordings matched our usual R_s constraints for absolute amplitude comparison in long-term recordings. Amplitudes remained comparable in a preliminary analysis of absolute amplitude values of evoked potentials in these (**Supplementary Figure 2D**). This is in contrast to the amplitude increase both in s/mIPSCs evinced in this study and in eIPSCs of more mature neurons studied previously (Janach et al., 2020). Moreover, while the release probability for s/mIPSC increased, the one for eIPSC probably decreased upon IFN- γ addition, thereby masking the (postsynaptic) IFN- γ effects. Given this, as well as the lack of PPD under control conditions, evoked release might be constrained in immature GABAergic synapses.

To test whether NO might contribute to IFN- γ -induced paired-pulse facilitation, we recorded another series using the paired-pulse paradigm and observed whether NO donor SNAP has an effect on PPR. SNAP (300 μ M), applied for 5 min, did not alter the PPR at 100 or 50 ms ISI ($PPR100ms_{ctrl} = 1.0 \pm 0.1$ vs. $PPR100ms_{SNAP} = 1.0 \pm 0.1$, $p = 0.8$, paired t -test, $n = 9$, $N = 3$ and $PPR50ms_{ctrl} = 0.9 \pm 0.1$ vs. $PPR50ms_{SNAP} = 0.9 \pm 0.1$, $p = 0.8$, paired t -test, $n = 9$, $N = 3$; **Figures 5E,F**). As the PPR remained comparable under application of NO donor SNAP, we conclude that NO does not contribute to IFN- γ -mediated paired-pulse facilitation.

However, paired-pulse facilitation implies an increased capability of reliably transferring inhibition at higher frequencies (Luhmann et al., 2014). Following this, paired-pulse facilitation points to stronger inhibition at frequencies ≥ 10 Hz.

Interferon- γ constrained excitability in the developing cortex

There is an ongoing debate about whether GABA acts inhibitory or excitatory at the early stages of development. At least in mice of the first postnatal week, GABA_AR openings in L5 neurons lead predominantly to depolarizing currents (Rehms et al., 2008). This may drive specific patterns of activity in developing neuronal networks (Ben-Ari, 2002; Ben-Ari et al., 2007). However, hyperpolarizing GABA actions in the neocortex have also been seen in the first postnatal week (Daw et al., 2007). In any case, the opening of GABA_ARs, in addition to its effect on membrane voltage, mediates a drop in membrane resistance that shunts excitatory inputs (Staley and Mody, 1992). Therefore, even "depolarizing" actions can (1) be considered as inhibitory, (2) inhibit neuronal output *in silico* (Morita et al., 2006), and (3) suppress network activity *in vivo* (Kirmse et al., 2015).

We here aimed at elucidating if and how the IFN- γ -induced increase in GABAergic transmission affects the developing cortical network. We therefore positioned brain slices on a microelectrode array (MEA, **Figure 6A**) and enhanced spontaneously occurring electrical events with 4-AP (50 μ M). IFN- γ attenuated the frequency of these events on average by a factor of 0.45 ± 0.09 within 15 min (from $f_{ctrl} = 22.6 \pm 4.3$ events min^{-1} to $f_{IFN-\gamma} = 9.4 \pm 2.8$ events min^{-1} , $p < 0.0001$, paired Wilcoxon signed-rank test, $n = 49$ distinguishable events, recorded in 8 slices from 6 animals, **Figures 6B,E**). This effect is GABA-mediated, as the frequency is not diminished upon IFN- γ when GABA_A receptors are blocked with bicuculline (10 μ M) (average factor 1.2 ± 0.2 , $f_{BMI} = 17.8 \pm 4.8$ events min^{-1} vs. $f_{BMI IFN-\gamma} = 10.9 \pm 2.9$ events min^{-1} , $p = 0.5$, paired Wilcoxon signed-rank test, $n = 30$ distinguishable events, recorded in 5 slices from 3 animals, **Figures 6D,E**). Because our patch clamp recordings imply that NO elevated spontaneous GABA release upon IFN- γ application, we next tested if IFN- γ attenuates network activity when NO production was inhibited. In the presence of 1400W (10 μ M), IFN- γ attenuated the frequency of events on average by a factor of 0.84 ± 0.13 ($f_{1400W} = 48.3 \pm 10.6$ events min^{-1} vs. $f_{1400W IFN-\gamma} = 31.1 \pm 5.8$ events min^{-1} , $p < 0.0001$, Wilcoxon signed-rank test, $n = 77$ distinguishable events, recorded in 8 slices from 3 animals **Figures 6C,E**). However, 1400W significantly reduces the effect size ($p < 0.0001$, Kruskal-Wallis ANOVA, performed on relative change factors **Figure 6E**). Note that the absolute event numbers largely depended on experimental conditions of each individual slice, thus enabling only longitudinal paired comparison. The Ca²⁺-dependent stimulation of transmitter release by 4-AP applies to both glutamatergic and GABAergic synapses: however, the effect of 4-AP enhanced release of GABA might be countered by the inhibition of postsynaptic GABA currents (Gu et al., 2004), thereby enabling the overall pro-excitatory effect of 4-AP. Both effects theoretically could mask

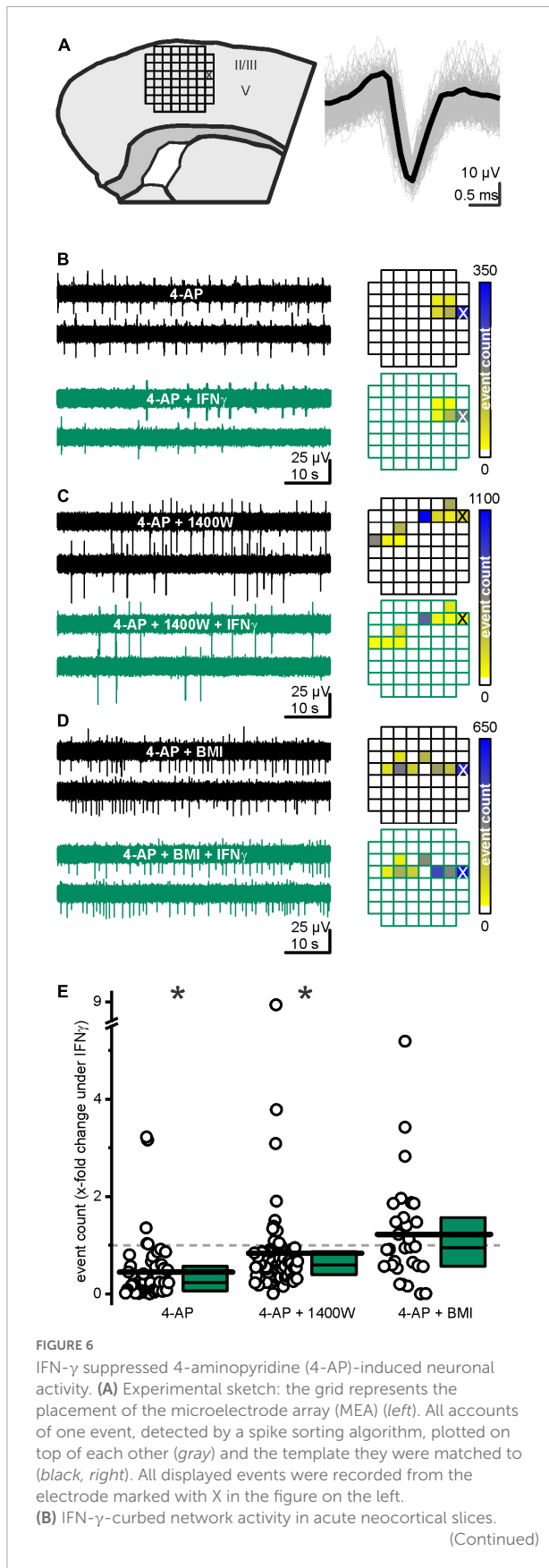


FIGURE 6
 Sample traces (left) recorded from the same electrode (marked with X in the heatmap below) before (black) and under (green) IFN- γ application. (C) Continuous iNOS inhibition via 1400W (10 μ M) partly prevented IFN- γ -mediated network activity suppression. (D) IFN- γ required functioning GABA_A receptors to curb network activity. Under continuous bicuculline methiodide (BMI, 10 μ M) application, IFN- γ failed to significantly alter event count. Example traces on top and exemplary heatmap below. (E) Relative event count change upon IFN- γ application in the absence of blockers and with 1400W or BMI, respectively. Most events considerably decreased in frequency upon IFN- γ . This attenuation is partly prevented in presence of 1400W and absent in the presence of BMI. Top, middle, and bottom lines of boxes represent percentiles 75, 50, and 25, respectively, and long bars represent means. * $p < 0.05$.

the sIPSC enhancement by IFN- γ . However, this would lead to an underestimation of the effect.

In summary, IFN- γ attenuates neocortical activity, i.e., it exerts network inhibition by constraining the occurrence of spontaneous events in a partly NO-dependent manner.

Discussion

Combining measurements at the single cell and network level, we herein have found that, during a period of GABA-dependent cortical maturation, IFN- γ acutely increases the frequency and amplitude of GABAergic IPSCs on neocortical pyramidal neurons. This effect was not reversible within 30 min. The increase in IPSC frequency is not a result of enhanced interneuron excitability, since interneuronal sub- and suprathreshold excitability parameters remained stable, and elevated IPSC frequency was still present under action potential suppression. We have identified iNOS and sGC as mediators of increased IPSC frequency upon IFN- γ , plausibly acting through elevated levels of NO. Notably, manipulations of the iNOS-NO-sGC pathway revealed a differential effect on frequency and amplitude, i.e., a specificity of NO for the putatively pre-synaptically mediated frequency increase. Together with the apparent separation of the IFN- γ effects on the frequency and amplitude of IPSCs, the cessation of IPSC amplitude increases when PKC was blocked postsynaptically argues against an increased GABA_AR sensitivity that might have uncovered subthreshold events from the noise. However, we cannot entirely exclude a contribution of synaptic modifications (i.e., an increased number of release sites) to the effect. Additionally, IFN- γ alters presynaptic function by shifting paired-pulse ratios toward facilitation. In contrast to the effect of IFN- γ on IPSCs, the effect on short-term synaptic plasticity was not dependent on NO. Functionally, IFN- γ constrains network activity in a GABA- and partially NO-dependent manner.

These new findings expand our existing knowledge of the neuromodulatory effects of IFN- γ on GABAergic transmission.

The increase in s/mIPSC amplitude that we observed here resembles the one that we have previously observed in adult and late juvenile rats (Janach et al., 2020). There we identified PKC-dependent increase in postsynaptic GABA_A receptor number as an underlying mechanism mainly by peak-scaled non-stationary noise analysis (Janach et al., 2022). Non-stationary noise analysis, however, is difficult to apply in developing systems because it requires many low rise time IPSCs, but immature synaptic integration results in comparatively low IPSC frequencies. We have here found, however, that PKC inhibitor Calphostin C, when added to the postsynaptic neuron, prevented increased amplitudes upon IFN- γ addition. This, in addition to a comparable effect size, led us to conclude that the mechanism for amplitude increase resembles the one we found in more mature neurons. Therefore, we did not attempt to investigate whether NO-mediated postsynaptic mechanisms, such as PKG-dependent phosphorylation (McDonald and Moss, 1994; Robello et al., 1996), or whether the altered expression of GABA receptor subunits and Cl⁻ co-transporters that were reported in early life inflammation (Reid et al., 2013) contribute to, or counteract with, the s/mIPSC amplitude increases.

Instead, we have here focused on a developmental peculiarity in the neocortex of P6–7 rats, namely, the IFN- γ induced increase in IPSC frequency. Although, in retrospect, a trend toward an increase in IPSC frequency might become apparent in more mature animals (Janach et al., 2020, 2022), this was rather inconsistent. Why does IFN- γ cause a robust and reliable increase in IPSC frequency early postnatal but much less later? There are several plausible explanations. (1) Active heterodimers of the sGC (that we herein have recognized as necessary for the IPSC frequency increase) are more prevalent in young rats than in adult rats (Haase et al., 2010). (2) As microglia in early brain development are in an activated state and gradually inactivate by P10 (Hristova et al., 2010), they constitutively express iNOS (Crain et al., 2013) that enables mechanisms to rapidly increase NO other than *via de novo* iNOS synthesis (that takes 12 h; Jiang et al., 2022). Such mechanisms include both substrate and cofactor availability (for review, see Cinelli et al., 2020). This scenario is in line with the rather long IFN- γ exposure necessary for increased IPSC frequencies in hippocampal neurons of more mature animals (Brask et al., 2004). (3) Functional synapses on pyramidal cells in early development may originate from interneurons disparate to those seen at later stages. For instance, certain early generated somatostatin expressing interneurons are more likely to form functional synapses with pyramidal neurons around P5–7 in mice (Wang et al., 2019), and the presynaptic response to IFN- γ might be subtype-specific. However, our analysis of mIPSC rise times might suggest a slight preference for perisomatic synapses in the IFN- γ effect on spontaneous release probability.

In line with our pharmacological evidence that iNOS is involved in IFN- γ -induced frequency change, NOS blockage has been shown to prevent an IFN- γ -induced IPSC frequency

increase (Brask et al., 2004) and IFN- γ slows γ -oscillations in an iNOS-dependent manner in organotypic hippocampal culture (Ta et al., 2019). In contrast to the tightly regulated, Ca²⁺-dependent, precise, and short-ranged nNOS action (Hardingham et al., 2013), iNOS can produce large amounts of NO independent of Ca²⁺ (Cinelli et al., 2020), plausibly enabling widespread multisynaptic actions. Regardless of the actual source, NO has been shown to increase IPSC frequency not only in the cortex (Wang et al., 2017) but also in the thalamus (Yang and Cox, 2007) and in the paraventricular nucleus (Li et al., 2004). Our data indicate that sGC is a prerequisite for the IFN- γ effect, therefore favoring a scenario in which NO impacts GABA release *via* downstream sGC targets (for review Hardingham et al., 2013). One of these putative targets, the hyperpolarization-activated cyclic nucleotide-gated cation (HCN) channel is involved in enhancing GABA release (Kopp-Scheinflug et al., 2015; Wang et al., 2017). HCN channels are present in cortical GABAergic boutons but their role may be more complex because blocking them also increases IPSC frequency (Cai et al., 2021). However, the PKC-mediated attenuation of HCN that we have previously seen upon type-I and II interferon application (Reetz et al., 2014; Janach et al., 2020), as well as direct activation of release machinery by PKC (Yawo, 1999; Xu et al., 2014), would be incompatible both with the lack of IPSC frequency increase when sGC was blocked (Figure 4B) and with findings in the central amygdala where PKC ϵ suppressed GABA release (Bajo et al., 2008). Other feasible sGC targets that could influence GABA release include P/Q Ca²⁺ channels as identified in brainstem neurons (Tozer et al., 2012) and faster vesicle recycling (Micheva et al., 2003). Again, NO-related mechanisms upstream of sGC, such as directly influencing L-Type Ca²⁺ channels (Tozer et al., 2012) or nitrosylation of release machinery proteins (Palmer et al., 2008), are less likely involved here. Rather, sGC-independent mechanisms inhibited cortical P/Q Ca²⁺ channels (Petzold et al., 2008). Further, the block of α -amino-3-hydroxy-5-methyl-4-isoxazolepropionic acid (AMPA) and NMDA receptors throughout our experiments excluded a contribution of directly NO-modulated NMDA (Dawson et al., 1996) or IFN- γ -increased AMPA Ca²⁺ conductance (Mizuno et al., 2008). NO may still induce Ca²⁺ release from intracellular sources as seen in striatal neurons (Horn et al., 2002). Taken together, we cannot rule out NO-mediated increase in presynaptic Ca²⁺, a classical modulator of transmitter release. Moreover, NO (donors) may elevate IPSC frequency Ca²⁺ independently (Li et al., 2004).

A parsimonious explanation of the obvious differences in the IFN- γ effect on s/mIPSCs and eIPSCs would be differential regulation of spontaneous and evoked GABA release by IFN- γ application indirectly implying segregation of the mechanisms underlying these two forms of vesicle release (Horvath et al., 2020). A plausible scenario for the peculiarities in evoked release would be that IFN- γ -mediated Ca²⁺ elevation might

meet a relative lack of slow-binding Ca^{2+} buffer parvalbumin (PV) in the boutons of early postnatal interneurons (del Rio et al., 1994). The latter may decelerate the decay of residual Ca^{2+} (Caillard et al., 2000). This hypothesis awaits further experimental examination.

The relative lack of PPD combined with a large variance of PPRs evinced in our sample when compared with PPD obtained under the same conditions in more mature animals (Supplementary Figure 2F; see also Xiang et al., 2002), is an incidental but interesting finding that is possibly linked to inhibitory synapse development.

IFN- γ -mediated changes certainly interfere with the complex role GABA is playing in neocortical development. Although the actual outcome is hard to predict, a transient alteration in GABAergic (or glutamatergic) signaling during cortical development can lead to persisting changes (Kaindl et al., 2008; Stefovská et al., 2008). Balanced GABA is crucial for adequate neuronal stem cell proliferation, cell migration, and synaptogenesis (for review, Wang and Kriegstein, 2009). Increased GABAergic signaling enhances interneuron apoptosis, curbs network synchrony (Duan et al., 2020), and causes GABA synapse elimination (Wu et al., 2012). GABAergic interneurons control critical periods of synaptic plasticity in functional circuits of the cortex (for review Hensch, 2005), i.e., enhanced GABAergic transmission prematurely induces such periods (Fagiolini et al., 2004), leading to a mismatch of sensory stimuli and synaptic plasticity. In line with this, transient disturbances of interneuron generation and integration cause long-term behavioral abnormalities—even after cell counts normalize (Magno et al., 2021). On one hand, excitation–inhibition balance is stabilized by GABAergic currents adapting to activity (Xue et al., 2014) but also sensory deprivation may increase GABAergic inhibition (Maffei et al., 2006). On the other hand, in our study, GABAergic transmission induced by IFN- γ led to an overall reduced spontaneous activity, which, in a period of incomplete synaptogenesis, may lead to decreased excitatory synaptic integration (Burrone et al., 2002).

The neuroimmune interaction we describe here might have clinical implications as altered GABAergic transmission is associated with neurodevelopmental disorders (Deidda et al., 2014). Even in the absence of disease, transient pharmacological increase in GABAergic transmission in juvenile mice not only leads to anxiety-related behavior in adults (Shen et al., 2012) but also normalizes disturbed social preferences in IFN- γ deficient mice (Filiano et al., 2016). In ASD, IFN- γ is notably the most pronounced among commonly elevated pro-inflammatory cytokines (reviewed in Saghazadeh et al., 2019) and children with ASD have elevated nitrate plasma levels that correlate with levels of IFN- γ but not with other cytokines (Sweeten et al., 2004). Alcohol dependence increases IFN- γ production in brain immune cells, as well as mIPSC frequency in the central amygdala that normalizes upon application of the anti-inflammatory cytokine interleukin 10 (Patel et al., 2021).

Our findings shed light on the acute effects of IFN- γ on early GABAergic transmission thus providing a mechanism for how early inflammation could interfere with cortical development. This might have far-reaching consequences because functional disturbances in early microcircuits lead to aberrant cortical wiring at later stages that may cause neurological or psychiatric conditions (Molnár et al., 2020).

Data availability statement

The original contributions presented in this study are included in the article/Supplementary material, further inquiries can be directed to the corresponding author.

Ethics statement

The animal study was reviewed and approved by the European Communities Council Directive of September 22nd, 2010 (2010/63/EU) under the licenses T 0212/14, T-CH 0034/20 for wildtype rats and T0215/11 for transgenic rats.

Author contributions

ND and US conceptualized the study and wrote the manuscript. ND performed and analyzed patch clamp recordings and *post hoc* stainings. AF supervised, analyzed, and contributed to MEA recordings. GJ, EB, and US contributed to patch clamp recordings. All authors contributed to the article and approved the submitted version.

Funding

We thank the Antje-Bürgel Stiftung and the Berlin Institute of Health for supporting ND and GJ with individual grants, respectively. EB was funded by the Ministry of Science and Higher Education of the Russian Federation Academic Excellence Program “priority-2030” of Lobachevsky University until February 2022.

Acknowledgments

We thank P. Lange and C.V. Braun for coding assistance, S. Grosser for microscopy instructions, A. Schädlich for

contributing to MEA recordings, J. König and R. Dannenberg for technical assistance. Special thanks go to Michael Depew for critical comments and language editing. VGAT-Venus transgenic rats were generated by Drs. Y. Yanagawa, M. Hirabayashi, and Y. Kawaguchi in National Institute for Physiological Sciences, Okazaki, Japan, using pCS2-Venus provided by A. Miyawaki.

Conflict of interest

The authors declare that the research was conducted in the absence of any commercial or financial relationships that could be construed as a potential conflict of interest.

References

- Alderton, W. K., Cooper, C. E., and Knowles, R. G. (2001). Nitric oxide synthases: Structure, function and inhibition. *Biochem. J.* 357, 593–615. doi: 10.1042/0264-6021:3570593
- Arolt, V., Rothermundt, M., Wandinger, K. P., and Kirchner, H. (2000). Decreased in vitro production of interferon-gamma and interleukin-2 in whole blood of patients with schizophrenia during treatment. *Mol. Psychiatry* 5, 150–158. doi: 10.1038/sj.mp.4000650
- Bajo, M., Cruz, M. T., Siggins, G. R., Messing, R., and Roberto, M. (2008). Protein kinase C epsilon mediation of CRF- and ethanol-induced GABA release in central amygdala. *Proc. Natl. Acad. Sci. U.S.A.* 105, 8410–8415. doi: 10.1073/pnas.0802302105
- Ben-Ari, Y. (2002). Excitatory actions of GABA during development: The nature of the nurture. *Nat. Rev. Neurosci.* 3, 728–739. doi: 10.1038/nrn920
- Ben-Ari, Y., Gaiarsa, J. L., Tyzio, R., and Khazipov, R. (2007). GABA: A pioneer transmitter that excites immature neurons and generates primitive oscillations. *Physiol. Rev.* 87, 1215–1284. doi: 10.1152/physrev.00017.2006
- Blanchette, J., Jaramillo, M., and Olivier, M. (2003). Signalling events involved in interferon- γ -inducible macrophage nitric oxide generation. *Immunology* 108, 513–522. doi: 10.1046/j.1365-2567.2003.01620.x
- Bortone, D., and Polleux, F. (2009). KCC2 expression promotes the termination of cortical interneuron migration in a voltage-sensitive calcium-dependent manner. *Neuron* 62, 53–71. doi: 10.1016/j.neuron.2009.01.034
- Brask, J., Kristensson, K., and Hill, R. H. (2004). Exposure to interferon- γ during synaptogenesis increases inhibitory activity after a latent period in cultured rat hippocampal neurons. *Eur. J. Neurosci.* 19, 3193–3201. doi: 10.1111/j.0953-816X.2004.03445.x
- Bruns, R. F., Miller, F. D., Merriman, R. L., Howbert, J. J., Heath, W. F., Kobayashi, E., et al. (1991). Inhibition of protein kinase C by calphostin C is light-dependent. *Biochem. Biophys. Res. Commun.* 176, 288–293. doi: 10.1016/0006-291X(91)90922-T
- Burrone, J., O'Byrne, M., and Murthy, V. N. (2002). Multiple forms of synaptic plasticity triggered by selective suppression of activity in individual neurons. *Nature* 420, 414–418. doi: 10.1038/nature01242
- Cai, W., Liu, S.-S., Li, B.-M., and Zhang, X.-H. (2021). Presynaptic HCN channels constrain GABAergic synaptic transmission in pyramidal cells of the medial prefrontal cortex. *Biol. Open* 11:bio058840. doi: 10.1242/bio.058840
- Caillard, O., Moreno, H., Schwaller, B., Llano, I., Celio, M. R., and Marty, A. (2000). Role of the calcium-binding protein parvalbumin in short-term synaptic plasticity. *Proc. Natl. Acad. Sci. U.S.A.* 97, 13372–13377. doi: 10.1073/pnas.230362997
- Cinelli, M. A., Do, H. T., Miley, G. P., and Silverman, R. B. (2020). Inducible nitric oxide synthase: Regulation, structure, and inhibition. *Med. Res. Rev.* 40, 158–189. doi: 10.1002/med.21599
- Clark, D. N., Begg, L. R., and Filiano, A. J. (2022). Unique aspects of IFN- γ /STAT1 signaling in neurons. *Immunol. Rev.* 2, 1–18. doi: 10.1111/imr.13092
- Cobos, I., Calcagnotto, M. E., Vilaythong, A. J., Thwin, M. T., Noebels, J. L., Baraban, S. C., et al. (2005). Mice lacking Dlx1 show subtype-specific loss of interneurons, reduced inhibition and epilepsy. *Nat. Neurosci.* 8, 1059–1068. doi: 10.1038/nn1499
- Crain, J. M., Nikodemova, M., and Watters, J. J. (2013). Microglia express distinct M1 and M2 phenotypic markers in the postnatal and adult central nervous system in male and female mice. *J. Neurosci. Res.* 91, 1143–1151. doi: 10.1002/jnr.23242
- Daw, M. I., Ashby, M. C., and Isaac, J. T. R. (2007). Coordinated developmental recruitment of latent fast spiking interneurons in layer IV barrel cortex. *Nat. Neurosci.* 10, 453–461. doi: 10.1038/nn1866
- Dawson, V. L., Kizushi, V. M., Huang, P. L., Snyder, S. H., and Dawson, T. M. (1996). Resistance to neurotoxicity in cortical cultures from neuronal nitric oxide synthase-deficient mice. *J. Neurosci.* 16, 2479–2487. doi: 10.1523/jneurosci.16-08-02479.1996
- Deidda, G., Bozarth, I. F., and Cancedda, L. (2014). Modulation of GABAergic transmission in development and neurodevelopmental disorders: Investigating physiology and pathology to gain therapeutic perspectives. *Front. Cell. Neurosci.* 8:119. doi: 10.3389/fncel.2014.00119
- del Rio, J., de Lecea, L., Ferrer, I., and Soriano, E. (1994). The development of parvalbumin-immunoreactivity in the neocortex of the mouse. *Dev. Brain Res.* 81, 247–259. doi: 10.1016/0165-3806(94)90311-5
- Ding, J. D., Burette, A., and Weinberg, R. J. (2005). Expression of soluble guanylyl cyclase in rat cerebral cortex during postnatal development. *J. Comp. Neurol.* 485, 255–265. doi: 10.1002/cne.20494
- Duan, Z. R. S., Che, A., Chu, P., Modol, L., Bollmann, Y., Babij, R., et al. (2020). GABAergic restriction of network dynamics regulates interneuron survival in the developing cortex. *Neuron* 105, 75.e–92.e. doi: 10.1016/j.neuron.2019.10.008
- Fagiolini, M., Fritschy, J. M., Löw, K., Möhler, H., Rudolph, U., and Hensch, T. K. (2004). Specific GABA circuits for visual cortical plasticity. *Science* 303, 1681–1683. doi: 10.1126/science.1091032
- Filiano, A. J., Xu, Y., Tustison, N. J., Marsh, R. L., Baker, W., Smirnov, I., et al. (2016). Unexpected role of interferon- γ 3 in regulating neuronal connectivity and social behaviour. *Nature* 535, 425–429. doi: 10.1038/nature18626
- Flood, L., Korol, S. V., Ekselius, L., Birnir, B., and Jin, Z. (2019). Interferon- γ potentiates GABA receptor-mediated inhibitory currents in rat hippocampal CA1 pyramidal neurons. *J. Neuroimmunol.* 337:577050. doi: 10.1016/j.jneuroim.2019.577050
- Garvey, E. P., Oplinger, J. A., Furfine, E. S., Kif, R. J., Laszlo, F., Whittle, B. J. R., et al. (1997). 1400W is a slow, tight binding, and highly selective inhibitor of inducible nitric-oxide synthase in vitro and in vivo. *J. Biol. Chem.* 272, 4959–4963. doi: 10.1074/jbc.272.8.4959

Publisher's note

All claims expressed in this article are solely those of the authors and do not necessarily represent those of their affiliated organizations, or those of the publisher, the editors and the reviewers. Any product that may be evaluated in this article, or claim that may be made by its manufacturer, is not guaranteed or endorsed by the publisher.

Supplementary material

The Supplementary Material for this article can be found online at: <https://www.frontiersin.org/articles/10.3389/fncel.2022.913299/full#supplementary-material>

- Giridharan, V. V., Réus, G. Z., Selvaraj, S., Scaini, G., Barichello, T., and Quevedo, J. (2019). Maternal deprivation increases microglial activation and neuroinflammatory markers in the prefrontal cortex and hippocampus of infant rats. *J. Psychiatr. Res.* 115, 13–20. doi: 10.1016/j.jpsychires.2019.05.001
- Gu, Y., Ge, S. Y., and Ruan, D. Y. (2004). Effect of 4-aminopyridine on synaptic transmission in rat hippocampal slices. *Brain Res.* 1006, 225–232. doi: 10.1016/j.brainres.2004.02.008
- Haase, N., Haase, T., Seanner, M., and Behrends, S. (2010). Nitric oxide sensitive guanylyl cyclase activity decreases during cerebral postnatal development because of a reduction in heterodimerization. *J. Neurochem.* 112, 542–551. doi: 10.1111/j.1471-4159.2009.06484.x
- Hardingham, N., Dachtler, J., and Fox, K. (2013). The role of nitric oxide in pre-synaptic plasticity and homeostasis. *Front. Cell. Neurosci.* 7:190. doi: 10.3389/fncel.2013.00190
- Hensch, T. K. (2005). Critical period plasticity in local cortical circuits. *Nat. Rev. Neurosci.* 6, 877–888. doi: 10.1038/nrn1787
- Horn, T. F. W., Wolf, G., Duffy, S., Weiss, S., Keilhoff, G., and MacVicar, B. A. (2002). Nitric oxide promotes intracellular calcium release from mitochondria in striatal neurons. *FASEB J.* 16, 1611–1622. doi: 10.1096/fj.02-0126com
- Horvath, P. M., Piazza, M. K., Monteggia, L. M., and Kavalali, E. T. (2020). Spontaneous and evoked neurotransmission are partially segregated at inhibitory synapses. *eLife* 9:e52852. doi: 10.7554/eLife.52852
- Hristova, M., Cuthill, D., Zbarsky, V., Acosta-Saltos, A., Wallace, A., Blight, K., et al. (2010). Activation and deactivation of periventricular white matter phagocytes during postnatal mouse development. *Glia* 58, 11–28. doi: 10.1002/glia.20896
- Ivashkiv, L. B. (2018). IFN γ : Signalling, epigenetics and roles in immunity, metabolism, disease and cancer immunotherapy. *Nat. Rev. Immunol.* 18, 545–558. doi: 10.1038/s41577-018-0029-z
- Janach, G. M. S., Böhm, M., Döhne, N., Kim, H.-R., Rosário, M., and Strauss, U. (2022). Interferon- γ enhances neocortical synaptic inhibition by promoting membrane association and phosphorylation of GABA_A receptors in a protein kinase C-dependent manner. *Brain. Behav. Immun.* 101, 153–164. doi: 10.1016/j.bbi.2022.01.001
- Janach, G. M. S., Reetz, O., Döhne, N., Stadler, K., Gresser, S., Byvaltcev, E., et al. (2020). Interferon- γ acutely augments inhibition of neocortical layer 5 pyramidal neurons. *J. Neuroinflammation* 17:69. doi: 10.1186/s12974-020-1722-y
- Jiang, X., He, H., Mo, L., Liu, Q., Yang, F., Zhou, Y., et al. (2022). Mapping the plasticity of morphology, molecular properties and function in mouse primary microglia. *Front. Cell. Neurosci.* 15:811061. doi: 10.3389/fncel.2021.811061
- Kaindl, A. M., Koppeltaetter, A., Nebrich, G., Stuwe, J., Siffringer, M., Zabel, C., et al. (2008). Brief alteration of NMDA or GABA_A receptor mediated neurotransmission has long term effects on the developing cerebral cortex. *Mol. Cell. Proteomics* 7, 2293–2310. doi: 10.1074/mcp.M800030-MCP200
- Kak, G., Raza, M., and Tiwari, B. K. (2018). Interferon-gamma (IFN- γ): Exploring its implications in infectious diseases. *Biomol. Concepts* 9, 64–79. doi: 10.1515/bmc-2018-0007
- Kang, Y., Dempo, Y., Ohashi, A., Saito, M., Toyoda, H., Sato, H., et al. (2007). Nitric oxide activates leak K⁺ currents in the presumed cholinergic neuron of basal forebrain. *J. Neurophysiol.* 98, 3397–3410. doi: 10.1152/jn.00536.2007
- Kavalali, E. T. (2015). The mechanisms and functions of spontaneous neurotransmitter release. *Nat. Rev. Neurosci.* 16, 5–16. doi: 10.1038/nrn3875
- Kirschchuk, S., Sinning, A., Blanquie, O., Yang, J.-W., Luhmann, H. J., and Kilb, W. (2017). Modulation of neocortical development by early neuronal activity: Physiology and pathophysiology. *Front. Cell. Neurosci.* 11:379. doi: 10.3389/fncel.2017.00379
- Kirmse, K., Kummer, M., Kovalchuk, Y., Witte, O. W., Garaschuk, O., and Holthoff, K. (2015). GABA depolarizes immature neurons and inhibits network activity in the neonatal neocortex in vivo. *Nat. Commun.* 6:7750. doi: 10.1038/ncomms8750
- Kopp-Scheinflug, C., Pigott, B. M., and Forsythe, I. D. (2015). Nitric oxide selectively suppresses IH currents mediated by HCN1-containing channels. *J. Physiol.* 593, 1685–1700. doi: 10.1113/jphysiol.2014.282194
- Kravchenko, M. O., Moskaliuk, A. O., Fedulova, S. A., and Veselovsky, N. S. (2006). Calcium-dependent changes of paired-pulse modulation at single GABAergic synapses. *Neurosci. Lett.* 395, 133–137. doi: 10.1016/j.neulet.2005.10.070
- Le Magueresse, C., and Monyer, H. (2013). GABAergic interneurons shape the functional maturation of the cortex. *Neuron* 77, 388–405. doi: 10.1016/j.neuron.2013.01.011
- Lee, J. J. (2009). Nitric oxide modulation of GABAergic synaptic transmission in mechanically isolated rat auditory cortical neurons. *Korean J. Physiol. Pharmacol.* 13, 461–467. doi: 10.4196/kjpp.2009.13.6.461
- Lewis, D. A., Hashimoto, T., and Volk, D. W. (2005). Cortical inhibitory neurons and schizophrenia. *Nat. Rev. Neurosci.* 6, 312–324. doi: 10.1038/nrn1648
- Lewis, E. L., Tulina, N., Anton, L., Brown, A. G., Porrett, P. M., and Elovitz, M. A. (2021). IFN γ -Producing $\gamma\delta$ T cells accumulate in the fetal brain following intrauterine inflammation. *Front. Immunol.* 12:741518. doi: 10.3389/fimmu.2021.741518
- Li, D. P., Chen, S. R., Finnegan, T. F., and Pan, H. L. (2004). Signalling pathway of nitric oxide in synaptic GABA release in the rat paraventricular nucleus. *J. Physiol.* 554, 100–110. doi: 10.1113/jphysiol.2003.053371
- Litteljohn, D., Nelson, E., and Hayley, S. (2014). IFN- γ differentially modulates memory-related processes under basal and chronic stressor conditions. *Front. Cell. Neurosci.* 8:391. doi: 10.3389/fncel.2014.00391
- Luhmann, H. J., Kirischuk, S., Sinning, A., and Kilb, W. (2014). Early GABAergic circuitry in the cerebral cortex. *Curr. Opin. Neurobiol.* 26, 72–78. doi: 10.1016/j.conb.2013.12.014
- Luhmann, H. J., and Prince, D. A. (1991). Postnatal maturation of the GABAergic system in rat neocortex. *J. Neurophysiol.* 65, 247–263. doi: 10.1152/jn.1991.65.2.247
- Maffei, A., Nataraj, K., Nelson, S. B., and Turrigiano, G. G. (2006). Potentiation of cortical inhibition by visual deprivation. *Nature* 443, 81–84. doi: 10.1038/nature05079
- Magno, L., Asgarian, Z., Pendolino, V., Velona, T., Mackintosh, A., Lee, F., et al. (2021). Transient developmental imbalance of cortical interneuron subtypes presages long-term changes in behavior. *Cell Rep.* 35:109249. doi: 10.1016/j.celrep.2021.109249
- McDonald, B. J., and Moss, S. J. (1994). Differential phosphorylation of intracellular domains of γ -aminobutyric acid type A receptor subunits by calcium/calmodulin type 2-dependent protein kinase and cGMP-dependent protein kinase. *J. Biol. Chem.* 269, 18111–18117. doi: 10.1016/s0021-9258(17)32424-9
- Micheva, K. D., Buchanan, J. A., Holz, R. W., and Smith, S. J. (2003). Retrograde regulation of synaptic vesicle endocytosis and recycling. *Nat. Neurosci.* 6, 925–932. doi: 10.1038/nn1114
- Mizuno, T., Zhang, G., Takeuchi, H., Kawanokuchi, J., Wang, J., Sonobe, Y., et al. (2008). Interferon- γ directly induces neurotoxicity through a neuron specific, calcium-permeable complex of IFN- γ receptor and AMPA GluR1 receptor. *FASEB J.* 22, 1797–1806. doi: 10.1096/fj.07-099499
- Modol, L., Bollmann, Y., Tressard, T., Babji, R., Che, A., Duan, Z. R. S., et al. (2020). Assemblies of perisomatic GABAergic neurons in the developing barrel cortex. *Neuron* 105, 93–105. doi: 10.1016/j.neuron.2019.10.007
- Molnár, Z., Luhmann, H. J., and Kanold, P. O. (2020). Transient cortical circuits match spontaneous and sensory-driven activity during development. *Science* 370:eabb2153. doi: 10.1126/science.abb2153
- Monteiro, S., Ferreira, F. M., Pinto, V., Roque, S., Morais, M., De Sá-Calc?da, D., et al. (2015). Absence of IFN γ promotes hippocampal plasticity and enhances cognitive performance. *Transl. Psychiatry* 5:e707. doi: 10.1038/tp.2015.194
- Monteiro, S., Roque, S., Marques, F., Correia-Neves, M., and Cerqueira, J. J. (2017). Brain interference: Revisiting the role of IFN γ in the central nervous system. *Prog. Neurobiol.* 156, 149–163. doi: 10.1016/j.pneurobio.2017.05.003
- Morita, K., Tsumoto, K., and Aihara, K. (2006). Bidirectional modulation of neuronal responses by depolarizing GABAergic inputs. *Biophys. J.* 90, 1925–1938. doi: 10.1529/biophysj.105.063164
- Müller, M., Fontana, A., Zbinden, G., and Gähwiler, B. H. (1993). Effects of interferons and hydrogen peroxide on CA3 pyramidal cells in rat hippocampal slice cultures. *Brain Res.* 619, 157–162. doi: 10.1016/0006-8993(93)91607-T
- Palmer, Z. J., Duncan, R. R., Johnson, J. R., Lian, L. Y., Mello, L. V., Booth, D., et al. (2008). S-nitrosylation of syntaxin 1 at Cys145 is a regulatory switch controlling Munc18-1 binding. *Biochem. J.* 413, 479–491. doi: 10.1042/BJ20080069
- Patel, R. R., Wolfe, S. A., Bajo, M., Abeynaike, S., Pahng, A., Borgonetti, V., et al. (2021). IL-10 normalizes aberrant amygdala GABA transmission and reverses anxiety-like behavior and dependence-induced escalation of alcohol intake. *Prog. Neurobiol.* 199:101952. doi: 10.1016/j.pneurobio.2020.101952
- Patterson, C. E., Lawrence, D. M. P., Echols, L. A., and Rall, G. F. (2002). Immune-mediated protection from measles virus-induced central nervous system disease is noncytolytic and gamma interferon dependent. *J. Virol.* 76, 4497–4506. doi: 10.1128/jvi.76.9.4497-4506.2002
- Petzold, G. C., Haack, S., Von Bohlen Und Halbach, O., Priller, J., Lehmann, T. N., Heinemann, U., et al. (2008). Nitric oxide modulates spreading

- depolarization threshold in the human and rodent cortex. *Stroke* 39, 1292–1299. doi: 10.1161/STROKEAHA.107.500710
- Pigott, B., Bartus, K., and Garthwaite, J. (2013). On the selectivity of neuronal NOS inhibitors. *Br. J. Pharmacol.* 168, 1255–1265. doi: 10.1111/bph.12016
- Pizzarelli, R., and Cherubini, E. (2011). Alterations of GABAergic signaling in autism spectrum disorders. *Neural Plast.* 2011:297153. doi: 10.1155/2011/297153
- Reetz, O., Stadler, K., and Strauss, U. (2014). Protein kinase C activation mediates interferon- β -induced neuronal excitability changes in neocortical pyramidal neurons. *J. Neuroinflammation* 11, 1–14. doi: 10.1186/s12974-014-0185-4
- Reid, A. Y., Riazi, K., Campbell Teskey, G., and Pittman, Q. J. (2013). Increased excitability and molecular changes in adult rats after a febrile seizure. *Epilepsia* 54, 45–48. doi: 10.1111/epi.12061
- Rheims, S., Minlebaev, M., Ivanov, A., Represa, A., Khazipov, R., Holmes, G. L., et al. (2008). Excitatory GABA in rodent developing neocortex in vitro. *J. Neurophysiol.* 100, 609–619. doi: 10.1152/jn.90402.2008
- Robello, M., Amico, C., Bucossi, G., Cupello, A., Rapallino, M. V., and Thellung, S. (1996). Nitric oxide and GABAA receptor function in the rat cerebral cortex and cerebellar granule cells. *Neuroscience* 74, 99–105. doi: 10.1016/0306-4522(96)00110-8
- Saghazadeh, A., Ataieina, B., Keynejad, K., Abdolizadeh, A., Hirbod-Mobarakeh, A., and Rezaei, N. (2019). A meta-analysis of pro-inflammatory cytokines in autism spectrum disorders: Effects of age, gender, and latitude. *J. Psychiatr. Res.* 115, 90–102. doi: 10.1016/j.jpsychires.2019.05.019
- Schindelin, J., Arganda-Carreras, I., Frise, E., Kaynig, V., Longair, M., Pietzsch, T., et al. (2012). Fiji: An open-source platform for biological-image analysis. *Nat. Methods* 9, 676–682. doi: 10.1038/nmeth.2019
- Schmidt, F. M., Lichtblau, N., Minkwitz, J., Chittka, T., Thormann, J., Kirkby, K. C., et al. (2014). Cytokine levels in depressed and non-depressed subjects, and masking effects of obesity. *J. Psychiatr. Res.* 55, 29–34. doi: 10.1016/j.jpsychires.2014.04.021
- Shen, Q., Fuchs, T., Sahir, N., and Luscher, B. (2012). GABAergic control of critical developmental periods for anxiety- and depression-related behavior in mice. *PLoS One* 7:e47441. doi: 10.1371/journal.pone.0047441
- Stadler, K., Bierwirth, C., Stoenica, L., Battenfeld, A., Reetz, O., Mix, E., et al. (2014). Elevation in type I interferons inhibits HCN1 and slows cortical neuronal oscillations. *Cereb. Cortex* 24, 199–210. doi: 10.1093/cercor/bhs305
- Staley, K. J., and Mody, I. (1992). Shunting of excitatory input to dentate gyrus granule cells by a depolarizing GABA(A) receptor-mediated postsynaptic conductance. *J. Neurophysiol.* 68, 197–212. doi: 10.1152/jn.1992.68.1.197
- Stefovska, V. G., Uckermann, O., Czuczwar, M., Smitka, M., Czuczwar, P., Kis, J., et al. (2008). Sedative and anticonvulsant drugs suppress postnatal neurogenesis. *Ann. Neurol.* 64, 434–445. doi: 10.1002/ana.21463
- Stuehr, D. J., and Marletta, M. A. (1987). Induction of nitrite/nitrate synthesis in murine macrophages by BCG infection, lymphokines, or interferon-gamma. *J. Immunol.* 139, 518–525.
- Sweeten, T. L., Posey, D. J., Shankar, S., and McDougle, C. J. (2004). High nitric oxide production in autistic disorder: A possible role for interferon- γ . *Biol. Psychiatry* 55, 434–437. doi: 10.1016/j.biopsych.2003.09.001
- Ta, T.-T., Dikmen, H. O., Schilling, S., Chausse, B., Lewen, A., Hollnagel, J.-O., et al. (2019). Priming of microglia with IFN- γ slows neuronal gamma oscillations in situ. *Proc. Natl. Acad. Sci.* 116, 4637–4642. doi: 10.1073/pnas.1813562116
- Tozer, A. J. B., Forsythe, I. D., and Steinert, J. R. (2012). Nitric oxide signalling augments neuronal voltage-gated L-type (Ca v1) and P/Q-type (Ca v2.1) channels in the mouse medial nucleus of the trapezoid body. *PLoS One* 7:1–7. doi: 10.1371/journal.pone.0032256
- Uematsu, M., Hirai, Y., Karube, F., Ebihara, S., Kato, M., Abe, K., et al. (2008). Quantitative chemical composition of cortical GABAergic neurons revealed in transgenic venus-expressing rats. *Cereb. Cortex* 18, 315–330. doi: 10.1093/cercor/bhm056
- Vetlugina, T. P., Lobacheva, O. A., Sergeeva, S. A., Nikitina, V. B., Nevidimova, T. I., and Semke, A. V. (2016). Adjunctive use of interferon γ inducer for treatment of patients with schizophrenia. *Acta Neuropsychiatr.* 28, 149–156. doi: 10.1017/neu.2015.60
- Wang, C. Z., Ma, J., Xu, Y. Q., Jiang, S. N., Chen, T. Q., Yuan, Z. L., et al. (2019). Early-generated interneurons regulate neuronal circuit formation during early postnatal development. *eLife* 8, 1–21. doi: 10.7554/eLife.44649
- Wang, D. D., and Kriegstein, A. R. (2008). GABA regulates excitatory synapse formation in the neocortex via NMDA receptor activation. *J. Neurosci.* 28, 5547–5558. doi: 10.1523/JNEUROSCI.5599-07.2008
- Wang, D. D., and Kriegstein, A. R. (2009). Defining the role of GABA in cortical development. *J. Physiol.* 587, 1873–1879. doi: 10.1113/jphysiol.2008.167635
- Wang, Q., Mergia, E., Koesling, D., and Mittmann, T. (2017). Nitric oxide/cGMP signaling via guanylyl cyclase isoform 1 modulates glutamate and GABA release in somatosensory cortex of mice. *Neuroscience* 360, 180–189. doi: 10.1016/j.neuroscience.2017.07.063
- Wu, X., Fu, Y., Knott, G., Lu, J., Di Cristo, G., and Josh Huang, Z. (2012). GABA signaling promotes synapse elimination and axon pruning in developing cortical inhibitory interneurons. *J. Neurosci.* 32, 331–343. doi: 10.1523/JNEUROSCI.3189-11.2012
- Xiang, Z., Huguenard, J. R., and Prince, D. A. (2002). Synaptic inhibition of pyramidal cells evoked by different interneuronal subtypes in layer V of rat visual cortex. *J. Neurophysiol.* 88, 740–750. doi: 10.1152/jn.2002.88.2.740
- Xu, C., Liu, Q. Y., and Alkon, D. L. (2014). PKC activators enhance GABAergic neurotransmission and paired-pulse facilitation in hippocampal CA1 pyramidal neurons. *Neuroscience* 268, 75–86. doi: 10.1016/j.neuroscience.2014.03.008
- Xue, M., Atallah, B. V., and Scanziani, M. (2014). Equalizing excitation-inhibition ratios across visual cortical neurons. *Nature* 511, 596–600. doi: 10.1038/nature13321
- Yang, S., and Cox, C. L. (2007). Modulation of inhibitory activity by nitric oxide in the thalamus. *J. Neurophysiol.* 97, 3386–3395. doi: 10.1152/jn.01270.2006
- Yawo, H. (1999). Protein kinase C potentiates transmitter release from the chick ciliary presynaptic terminal by increasing the exocytotic fusion probability. *J. Physiol.* 515, 169–180. doi: 10.1111/j.1469-7793.1999.169ad.x
- Yger, P., Spampinato, G. L. B., Esposito, E., Lefebvre, B., Deny, S., Gardella, C., et al. (2018). A spike sorting toolbox for up to thousands of electrodes validated with ground truth recordings in vitro and in vivo. *eLife* 7:e34518. doi: 10.7554/eLife.34518
- Zaqout, S., Blaesus, K., Wu, Y. J., Ott, S., Kraemer, N., Becker, L. L., et al. (2019). Altered inhibition and excitation in neocortical circuits in congenital microcephaly. *Neurobiol. Dis.* 129, 130–143. doi: 10.1016/j.nbd.2019.05.008